DOE/ET/33003--T4

JET PROPULSION LABORATORY
CALIFORNIA INSTITUTE OF TECHNOLOGY
PASADENA, CALIFORNIA

DISCLAIMER

DISCLAIMER

Portions of this document may be illegible in electronic image products. Images are produced from the best available original document.

900-755

DEGRADATION MODEL

FOR AN RTG

WITH A SILICON-GERMANIUM THERMOPILE

MASTER

AI03-76ET33003

EM 341-003-B September 1976

Prepared by

G. Stapfer
Thermal Energy Conversion Group

Approved by Vincent Truscello

Vincent C. Truscello, Supervisor
Thermal Energy Conversion Group

Jet Propulsion Laboratory
California Institute of Technology
Pasadena, California

DISTRIBUTION

Internal

R. J. Beale	122-123
F. M. Bell	277-102
G. Bodt	277-102
K. M. Dawson	198-102
R. F. Draper	233-307
R. L. Heacock	169-327
R. G. Ivanoff	277-102
H. L. Johnson	198-220
T. W. Koerner	198-220
E. L. Noon	277-102
P. Rouklove	277-102
J. L. Savino	198-102
W. S. Shipley	169-327
H. L. Steele	277-102
V. C. Truscello	277-102
P. Wiener	198-220
A. Zoltan	277-102
L. D. Zoltan	277-102

DISTRIBUTION

External

C. Alexander (BMI)

W. Barnett (Teledyne Isotopes)

R. Brouns (ERDA-NRA)

N. Elsner (GA)

E. F. Hampl, Jr. (3M Company)

L. Holcomb (NASA-OAST)

C. E. Kelly, Jr. (GE)

H. Kling (Fairchild)

A. Lieberman (Teledyne Isotopes)

J. W. McGrew (Teledyne Isotopes)

J. McKiernan (Sandia)

P. A. O'Riordan (ERDA-NRA)

V. Raag (Syncal)

H. Rauch (ERDA, SAN)

C. Rose (WANL)

A. C. Schaffhauser (Oak Ridge)

W. Von Flue (ERDA, SAN)

P. Waldron (Lincoln Lab)

W. W. Ward (Lincoln Lab)

ACKNOWLEDGMENTS

Much of this report deals with the analysis of data which are subsequently utilized and reduced in the Computer Code DEGRA. Special acknowledgment is therefore due to Mr. E. L. Noon who was responsible for the operation and coding of the computer. Thanks to his efforts large volumes of input and output data were reduced to meaningful tables and computerized plots.

The major technical contributors are the following:

G. Bodt

R. Caputo

E. L. Noon

V. Raag (Syncal Corp.)

G. Stapfer

V. C. Truscello

L. D. Zoltan

Additional credit is due to the MHW personnel of General Electric and RCA who were responsible for the successful development of the MHW generator and to ERDA which supported this work under the direction of Mr. P. O'Riordan, Office of Technical Development and Special Projects of the ERDA Division of Nuclear Research and Applications.

Particular acknowledgment is given to Dr. A. Mowery of ERDA who provided many hours of stimulating conversation on the subject of this report and helped us to focus on interpretation of results.

ABSTRACT

This report describes the RTG degradation mechanisms which have been identified as occurring in thermoelectric power generating systems that use the alloy of silicon germanium as the thermoelectric material and that incorporate a multifoil thermal insulation system. The synergetic effects of all of the identified degradation mechanisms are determined by a computer code, DEGRA, which calculates the available generator output power as a function of generator operating time.

CONTENTS

SECTION I

INTRODUCTION

A major objective of the extensive silicon germanium technology program which is drawing to its conclusion at JPL has been the development of the ability to predict the long-term performance behavior of a Radioisotope Thermoelectric Generator (RTG) using SiGe thermoelectric unicouples. The MJS77 project will use a set of three of these RTGs to provide all of the electrical power for spacecraft operation.

A number of degradation mechanisms, including thermoelectric property changes and chemical material interactions, in addition to the time dependent reduction in heat input caused by isotope decay, significantly reduce the available output power of an RTG over a four to six year mission. From the results of the many different types of basic material experiments which were conducted as part of the SiGe technology program, a total RTG degradation model was developed. This model, which has been computerized, allows the synergetic interactions of all of the degradation mechanisms to be determined and enables a realistic assessment of the available output power at any time.

This report discusses the basic data which make up the input or degradation parameters of the model. The basic thermoelectric generator performance model, i.e., the mathematical structure of the model, was previously documented in Reference 1. As the SiGe technology program progressed, it provided the necessary data which allowed an ever more realistic assessment of the degradation mechanisms. The model was periodically updated (References 2 through 5). The present report is the latest of these updates and represents the current performance projections of a Si_3N_4 coated SiGe thermoelectric generator.

SECTION II

DEGRADATION MECHANISMS

A number of mechanisms, most of which are time and temperature dependent, continuously alter the amount of power which is available from an RTG. Most of these mechanisms tend to reduce the output power of an RTG, hence the term degradation mechanisms. There are some mechanisms which actually increase the output power with time (a decreasing thermal conductivity of the SiGe alloy as an example). Some of these mechanisms have been well understood for some time and their effects on the generator output power have been accurately determined with a fair degree of confidence. On the other hand, there are mechanisms which have required considerable experimental data to be obtained and only recently have these effects on generator performance been predicted with any degree of accuracy.

Mechanisms of the first type are

a) Radioisotope Fuel Decay. The isotope fuel (Pu-238 in the case of the MHW generator), which is used to provide the thermal input power to the generator by isotopic decay, decreases as a function of the characteristic half life of the particular isotope which is being used. This change in the available thermal input power can readily be calculated, and its effect on the generator temperature and output power determined. The output power loss due to this mechanism constitutes the largest decrease of power attributable to a single mechanism (excepting catastrophic failures such as electrical shorts, etc.).

b) Thermoelectric Material Property Changes. The bulk thermoelectric material properties are time and temperature dependent and change according to a dopant precipitation model. This model has been described in detail (Ref. 3) and is based on the limited solubility of dopant (e.g., boron for

for the P material and phosphor for the N material) in the SiGe alloy. In parts of the thermoelectric legs (this part being temperature dependent) some of the original dopant comes out of solution, thus reducing the figure of merit (a parameter which measures the effectiveness with which the thermoelectric material converts thermal energy to electrical power) of the material as a function of operating time.

c) Material Sublimation. The unicouples are operated at elevated temperatures and dimensional changes due to sublimation can occur. Dimensional changes of the SiMo hot shoe as well as the SiGe thermoelectric legs change both the thermal and electrical performance of the thermopile. The rate of material sublimation has been determined experimentally, and with knowledge of the density of the material, the geometry changes can be calculated.

Analytical expressions describing the above three mechanisms are utilized in the DEGRA model which calculates the available output power as a function of operating time. However, in this report no further detailed description of these three degradation mechanisms are described.

Degradation mechanisms of the second type are the mechanisms which are detailed in this report. As was mentioned above, these mechanisms have only recently been sufficiently characterized to allow an accurate accounting of their contribution to the generator power loss. A large part of the data which is used to calculate the effects of these degradation mechanisms is based on the 18-couple module test program which has been conducted by RCA. These modules serve, to a large extent, as a data base for the performance prediction of the full generator. A variety of these modules have been operated over a range of temperatures, and in order to use this large amount of data a computer program was developed at JPL which allows the various parameters of the 18-couple modules to be correlated and effectively utilized (Ref. 6). Two degradation mechanisms in particular have been developed using the data accumulated from the 18-couple module test program. The mechanisms are (1) the decrease in electrical resistance between the unicouple and the thermal insulation foil package and (2) the change in thermal conductance of the multifoil thermal insulation. Both of these degradation mechanisms are time and temperature dependent, as they are primarily caused by chemical reaction products which deposit in the intermediate temperature regions of the thermopile. Later sections of this report will deal extensively with these two degradation mechanisms, showing the development of a unique parameter (the amount of silicon evaporating from specific regions of the unicouple), which enables the data correlation of modules operating at different temperatures and with and without a protective surface coating.

It had been suspected for a considerable period of time that the thermal conductivity of the SiGe thermoelectric alloy is not constant with time (although earlier degradation models assumed a constant thermal conductivity due to lack of conclusive data). As a result of experiments which were conducted at Syncal Corporation under contract to JPL, it was established that the thermal conductance of the SiGe alloy materials does indeed change with operating time. Although this change is in a direction (the thermal conductance is decreasing with time) which would normally improve the performance of the SiGe generator (because of a corresponding increase in operating temperature), this mechanism might cause further degradation effects to occur in the generator due to increased chemical reactions. The effect of this parameter is also discussed in the report.

The total resistance of a unicouple consists of several individual resistance terms. The DEGRA code utilizes the basic resistivity data of the SiGe alloy (these data are an input to the code) integrated over the applicable temperature gradient, and combines it with the unicouple leg geometry to obtain the total leg resistance. To this leg resistance, terms are added which represent the hot junction interface resistance, the hot shoe resistance and other extraneous contact resistances to obtain the total unicouple resistance. All of these various resistance terms are sensitive to temperature, and it was found (as experimental data become available) that the temperature sensitivity of the hot shoe and extraneous resistance terms which were used initially did not agree with the experimental data. The code was subsequently modified to include a better definition of the extraneous resistance, and a discussion of the results of these changes are included in the report.

After it became apparent that a large part of the generator degradation was caused by material sublimation, the unicouples were coated with silicon nitride (Si_3N_4); the coating acts as an effective combatant to this degradation mechanism. An extensive program was conducted at JPL to evaluate this coating and to obtain basic data such as material loss rates of coated silicon molybdenum and the lifetime of the coating. Experiments were conducted both in hard vacuum systems as well as in an environment of low pressure carbon monoxide. The CO experiments were necessary after it became evident that the CO had a deleterious effect on the lifetime of the Si_3N_4 coating. The effect of premature loss of the Si_3N_4 coating is, therefore, also included in the detailed description of the degradation mechanisms.

SECTION III

HOT SHOE BULK RESISTANCE CHANGE

The RTG performance model determines the total electrical resistance of a unicouple from the sum of a number of individual resistance terms, e.g., N and P leg resistance, hot shoe resistance, cold strap resistance, etc. One of these terms, designated as the extraneous resistance, is primarily utilized to match the total model resistance with the experimentally measured resistance of an RTG. During the early RTG performance modeling, this term was adjusted to match the experimental data of a single performance point (the only point available at the time). As more experimental data became available, it became apparent that the total resistance of an electrically heated generator (ETG) as a function of hot junction temperature varied in a manner quite different from that predicted by the model. The original model assumed that the extraneous resistance was a constant percent of the total leg resistance even as temperature varied. The experiments with the ETGs confirmed that this is not the case and that the extraneous resistance is a strong function of temperature, increasing with higher temperatures. The result of this behavior was that the code predicted an output power which was too high at temperatures above 1000^oC and an output power too low at temperatures below 1000^oC. The value of 1000^oC was the temperature at which experimental and model data were originally matched. However, at other temperatures the powers did not match. To account for this, the current model modifies the extraneous resistance term as a function of temperature. The result of this modificiation is compared with the original model in Figure 1. The graph shows the output power as a function of input power, thus in effect changing the operating temperature. The dashed line shows the output power based on the previous (unmodified) model while the solid line depicts the current version of the model. From the data in this figure it can be seen that the present

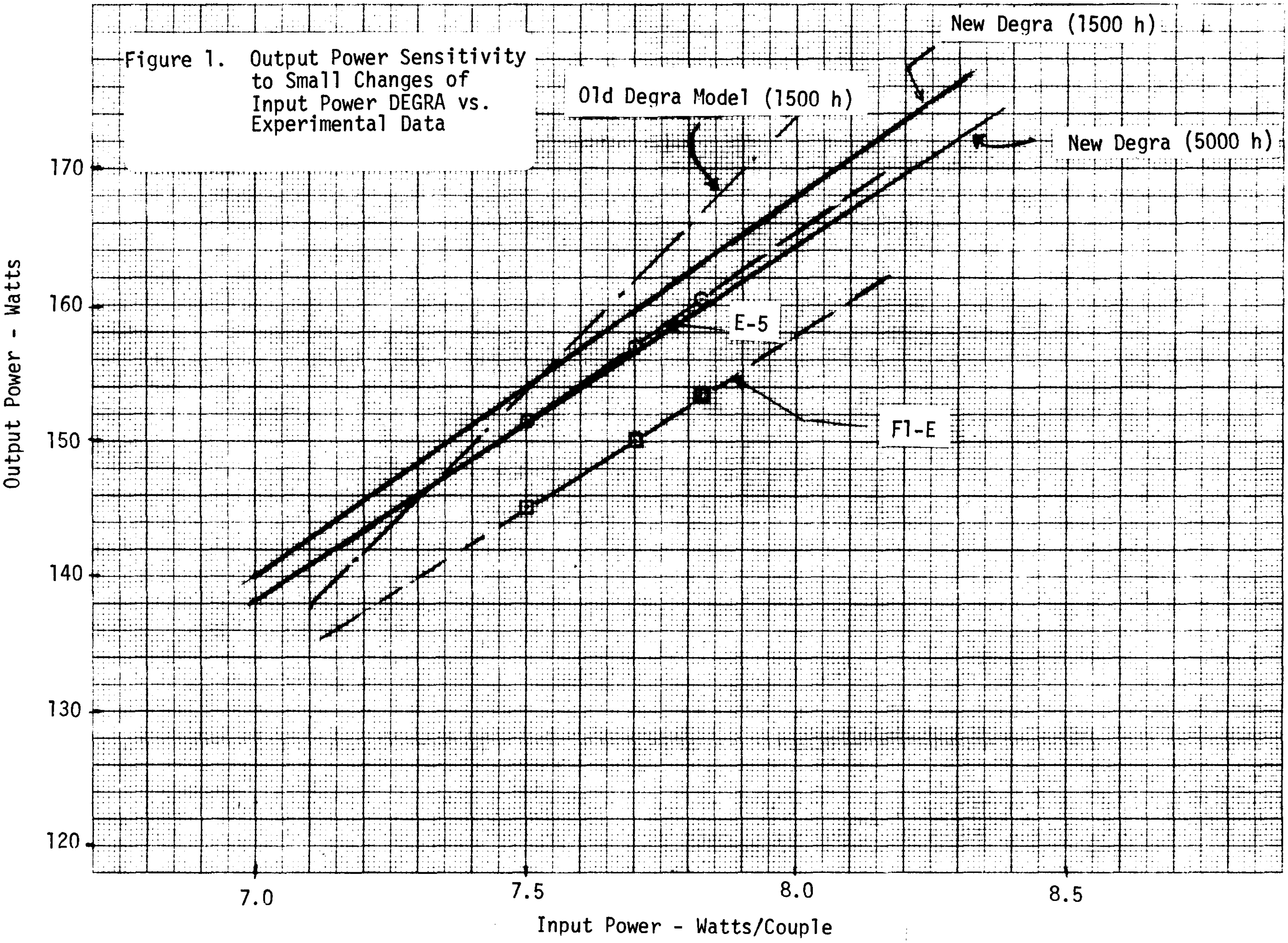

Figure 1. Output Power Sensitivity to Small Changes of Input Power DEGRA vs. Experimental Data

version of the model conforms very closely to the latest experimental ETG performance data, such as E-5 and F1-E, which are also shown in the figure.

SECTION IV

THE EFFECT OF A CHANGING THERMOELECTRIC MATERIAL THERMAL CONDUCTIVITY

The thermal conductivity of the SiGe alloy has in the past been assumed to be constant as a function of time, and only dependent upon temperature. This behavior became suspect, however, in the course of the 4-couple module program, and efforts were made to ascertain if, and if so at what rate, the thermal conductivity of the SiGe alloy was changing. At the Syncal Corporation, under contract to JPL, the thermal conductivity of the N and P type SiGe alloy was measured as a function of time as well as temperature. The technical details describing this experimental effort are documented in the JPL bimonthly progress reports which are submitted to the Energy Research and Development Administration (ERDA). The conclusions which can be drawn from these experiments are (1) the thermal conductivity of both the N and P doped alloys changes with time above a temperature of 700^{o}C, and (2) the thermal conductivity is constant with time at temperatures below 700^{o}C. The reason for the decrease in thermal conductivity above 700^{o}C is that an alloying of the not completely homogeneous material is taking place. (The reason for the decrease stems from the fact that both Si and Ge, in their elemental form, exhibit much larger values of thermal conductivity compared to a truly homogeneous SiGe alloy; a 75% Si - 25% Ge alloy exhibits the lowest value of conductivity.) The Syncal data analysis, which is supported by almost two years of lifetime data, accounts for the changing thermal conductance as a function of time. The extent of this change for the combined N and P material is shown in Figure 2 for three nominal hot junction - cold junction temperature intervals. As indicated in the figure, most of the change takes place during the initial two years of operation. It also shows that the change is much more pronounced with increased hot junction temperature.

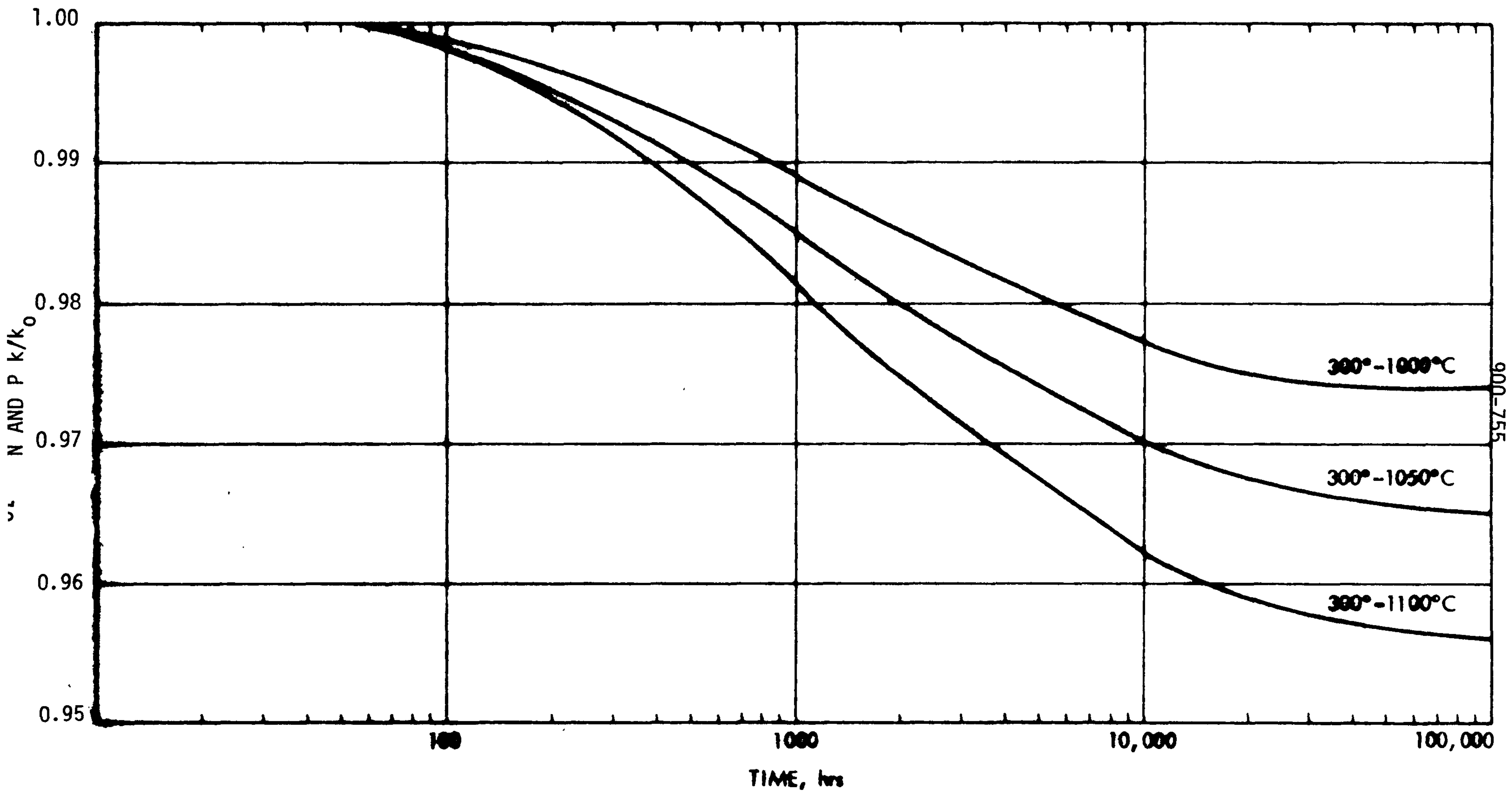

Figure 2. Time and Temperature Dependency of n and p-type SiGe Thermal Conductivity

The overall effect, which this variable thermal conductivity has on the performance capabilities of the SiGe thermoelectric material is shown in Figure 3. Depicted in this figure is the figure of merit (Z) of an N type SiGe alloy for different operating times. The effect of the thermal conductance change is seen at the 900^{0}-$1000^{0}C$ temperature range while the variation of Z with time at the lower temperatures (300^{0}-$700^{0}C$) are characteristically the dopant precipitation effects. A lowering of the thermal conductivity improves conversion efficiency and increases temperatures, however, too large an increase in operating temperature can result in greater material interactions and decreased power.

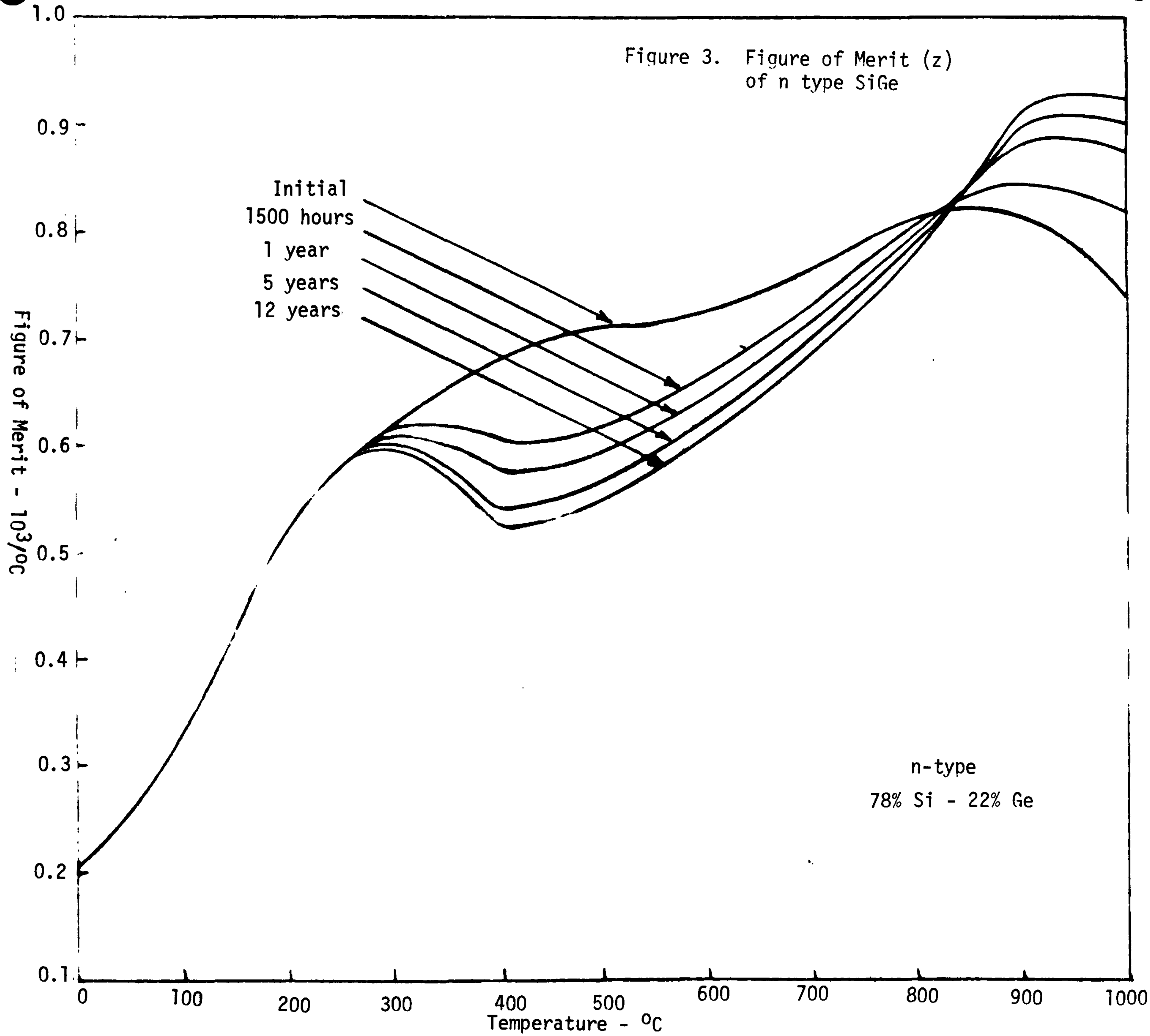

Figure 3. Figure of Merit (z) of n type SiGe

900-755

SECTION V

SILICON LOSS, A CORRELATING PARAMETER

Some generator degradation mechanisms, in particular the degradation of thermal insulation and the decreasing electrical shunt resistance, are sensitive to and strongly dependent upon operating temperatures. In order to determine the extent to which a given degradation mechanism will deteriorate the performance of an RTG over a four to six year mission using only relatively short testing times, experiments are performed over a range of temperatures. The results of these experiments require some common parameter in order to correlate and interpret the data. One parameter which was found to be useful for this purpose and which has been used in the past, is the amount of silicon which sublimes from the hot shoe. This same parameter is still used, but with the following modification. It has been found that only a portion of the silicon evaporating from the unicouple and reacting with the SiO_2 cloth will contribute to generator degradation. Figure 4 shows that portion of the SiGe leg and the SiMo hot shoe which actually contributes silicon for the degradation process. In the case of the leg, since the leg temperature decreases rapidly along its length, only the top (hottest) part of the leg sublimes significant amounts of silicon to react with the surrounding insulation cloth and thus produce silicon monoxide ($Si + SiO_2 \rightarrow 2SiO$). The silicon which sublimes from the hot shoe area facing the heat source does not contribute to the degradation since this silicon fully reacts with the graphite structure of the heat source. Likewise, the silicon from the edge of the hot shoe either reacts directly with the heat source or with the SiO_2 cloth near the hot shoe. This latter silicon produces SiO which in turn readily reacts with the graphite heat source. Little of this SiO reaches the leg area where degradation can occur. Most of the hot shoe's back side is baffled by the Al_2O_3 barrier piece, and thus very little of the

Figure 4. Sublimation Areas Considered for Degradation Contribution

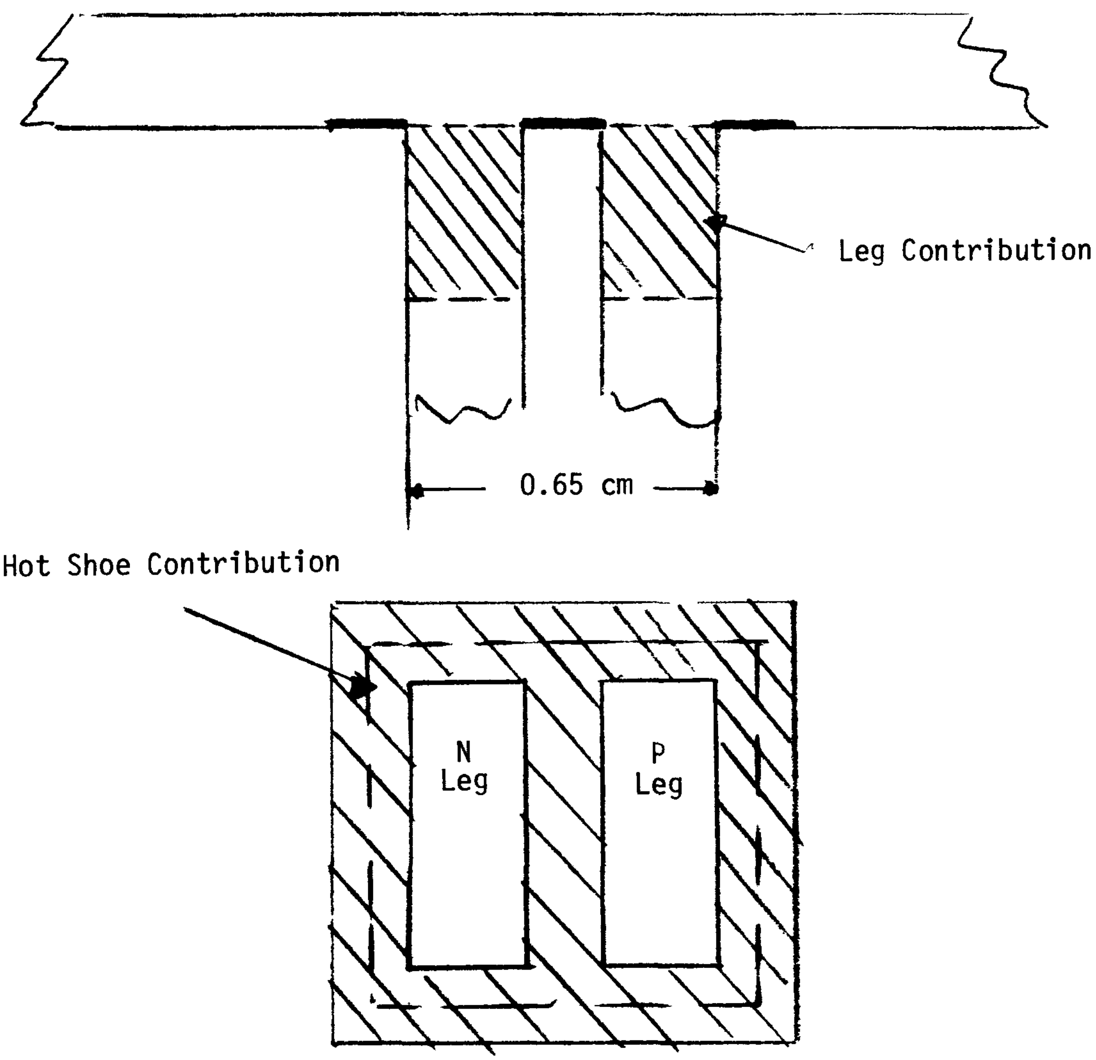

Area of Hot Shoe Contribution - 0.4 cm^2

Area of Leg Contribution - 0.6 cm^2 *

* The loss rate of Si_3N_4 coated SiGe is reduced by one decade with a temperature drop of about 60^oC. The temperature gradient along the unicouple leg is $35^oC/mm = 10^oC/0.1\ cm^2$.

reaction products will originate from this area. This leaves only a small area near the hot junction to be considered as shown in Figure 4. Silicon from this area will heavily contribute to the thermal insulation and shunt resistance degradation mechanisms. Based on these area considerations and experimentally determined loss rates for coated and uncoated SiMo and SiGe (Ref. 7), the silicon losses per unicouple which contribute to the degradation mechanisms have been calculated as a function of hot junction temperature and are shown in Figure 5. Two silicon loss rates are shown on the Arrhenius plot. The lower rate pertains to the Si_3N_4 coated unicouples while the larger rate pertains to uncoated unicouples.

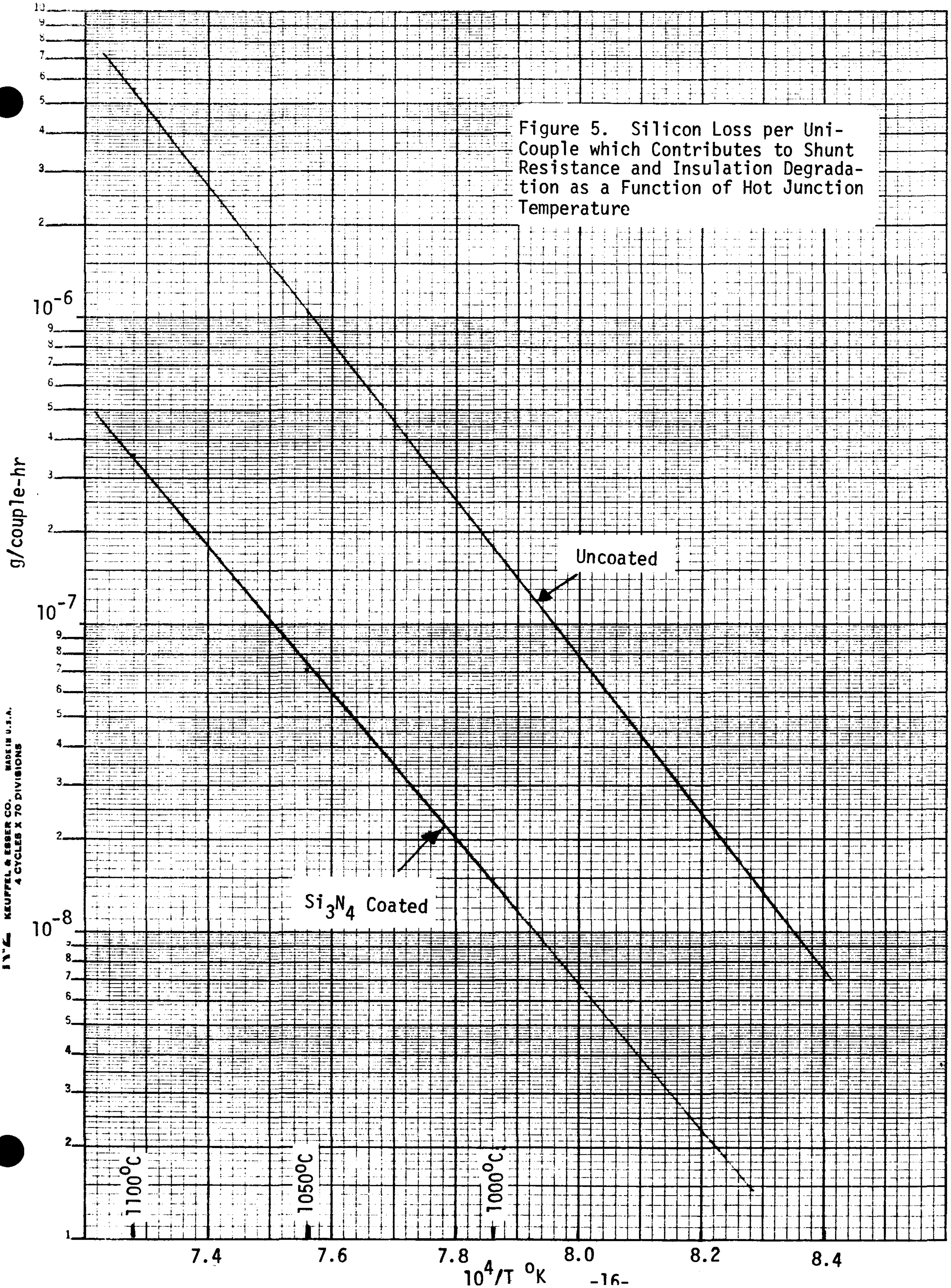

Figure 5. Silicon Loss per Uni-Couple which Contributes to Shunt Resistance and Insulation Degradation as a Function of Hot Junction Temperature

SECTION VI

DEGRADATION DUE TO CHANGE IN ELECTRICAL SHUNT RESISTANCE

A major advantage of the SiGe thermoelectric system over other thermoelectric systems is the ability to operate at relatively high temperatures, thus obtaining a high specific power output. However, this elevated temperature requires the use of a metallic multifoil thermal insulation system in order to achieve high efficiency. To prevent short circuiting of the thermoelectric legs by this metallic thermal insulation system, the unicouples are individually wrapped with electrically insulating astroquartz (SiO_2) yarn. Silicon, which sublimes at the elevated temperatures from the hot shoe and leg, reacts with the yarn and forms SiO ($Si + SiO_2 \rightarrow 2\ SiO$), which in its gaseous state diffuses along the unicouple legs through the astroquartz yarn toward the cooler regions of the system. At intermediate temperatures (approximately 600^{o}C) this gaseous SiO condenses, forming a porous solid between the unicouple legs and the adjacent multifoil insulation metal foils. The SiO disassociates into SiO_2 and Si. The electrically conductive Si sets up a shunting path between the unicouple and the foil, which in effect reduces the available generator output power. The lower the shunt resistance, the more energy is internally dissipated within the thermopile and the less energy is available as useful output.

One of the parameters which is measured as part of the normal data recording for nearly all of the SiGe test units (such as the 4-couple, 18-couple modules and ETGs) is the electrical shunt resistance. Depending upon the operating temperature and whether or not the unicouple is coated with Si_3N_4, the initial shunt resistance values as well as the onset of decrease with time will vary by orders of magnitude. However, it has been found that since the shunt resistance is directly attributable to the amount of silicon (SiO) which deposits along the wrap, it is possible to correlate all of the shunt resistance data to this common parameter (silicon loss from Figure 5). Figure 6 shows the shunt resistance for seven 18-couple modules which operated at hot shoe temperatures from as low as $985^{o}C$ (18-H) up to $1135^{o}C$ (18-K). All of these modules were uncoated, i.e., none used the Si_3N_4 coating which was developed later in the program to reduce the amount of silicon which sublimes. Figure 7 shows the shunt resistance for the 18-couple modules which do use the Si_3N_4 coating. The data from these two curves are combined in Figure 8, which shows the shunt resistance of all the 18-couple modules (coated and uncoated) as a function of silicon loss. Although some spread in these data still exists, a definite trend can be observed.

Three different rates of resistance change have been identified. These rates are (1) a low rate of change, (2) a high rate of change and (3) a nominal rate of change. Most of the modules are close to the nominal rate of change. In particular, SN-1 and 18-0 (the first two Si_3N_4 coated modules which operated at $1135^{o}C$) conform very well with the selected nominal rate of change curve. Only a few modules deviate greatly from the nominal and they formulate the high and low rate curves. Equations were derived for each of the three rate changes and are used in the DEGRA computer code to obtain their effects on the available generator output power.

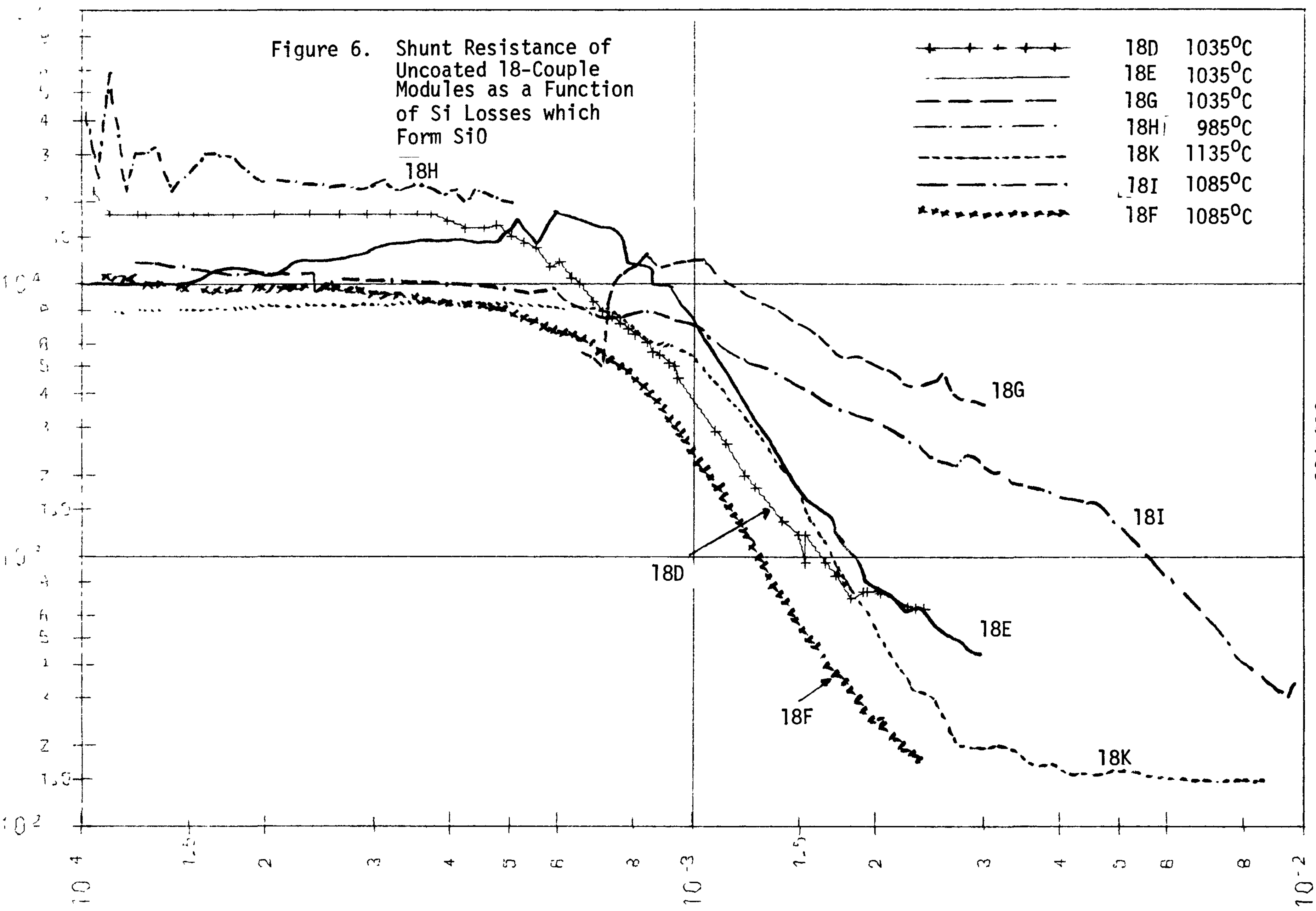

Figure 6. Shunt Resistance of Uncoated 18-Couple Modules as a Function of Si Losses which Form SiO
18D 1035°C
18E 1035°C
18G 1035°C
18H 985°C
18K 1135°C
18I 1085°C
18F 1085°C
18H
18G
18I
18D
18E
18F
18K
Foil Resistance - Ohms
Silicon - g/couple

900-755

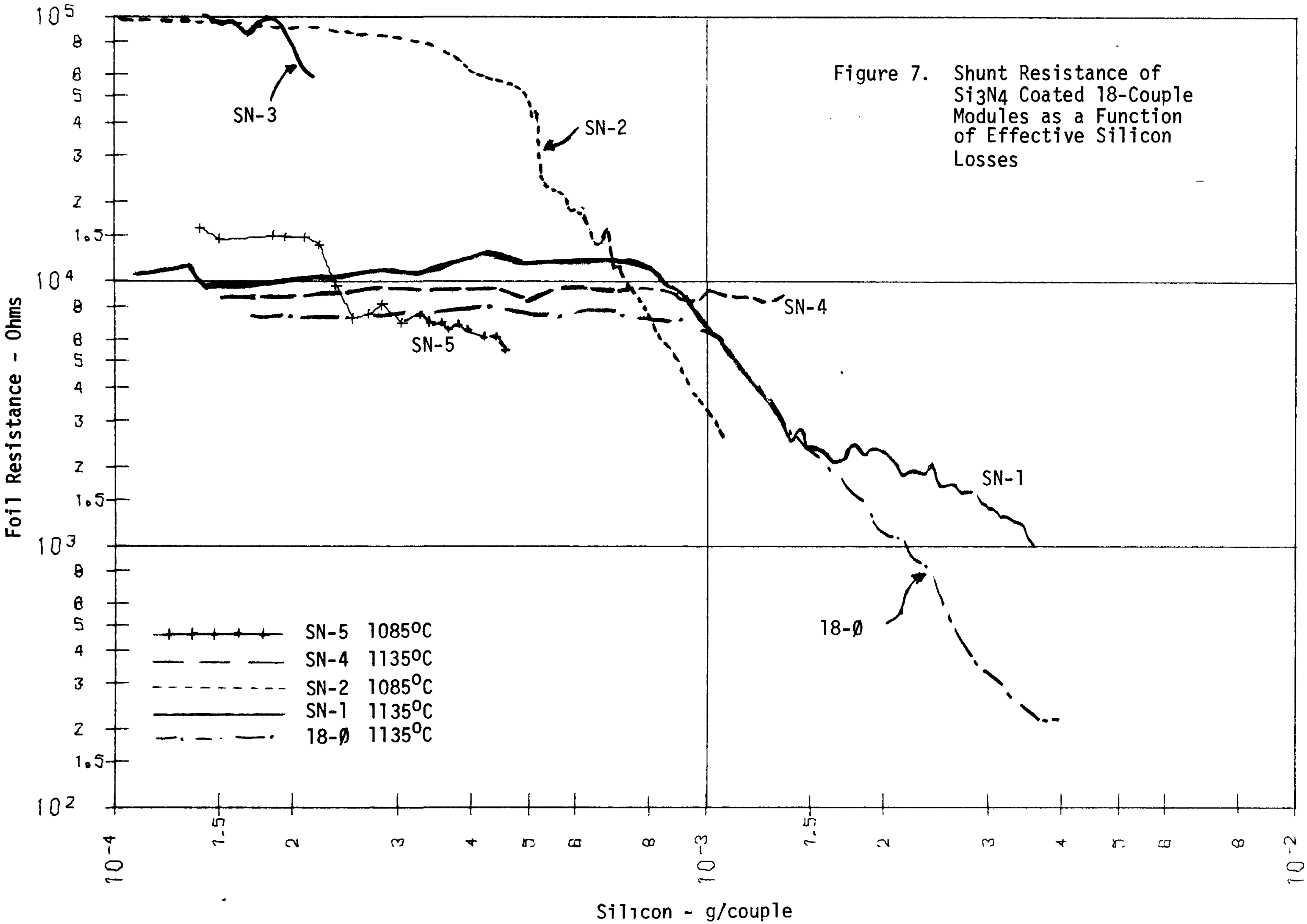

Figure 7. Shunt Resistance of Si_3N_4 Coated 18-Couple Modules as a Function of Effective Silicon Losses

900-755

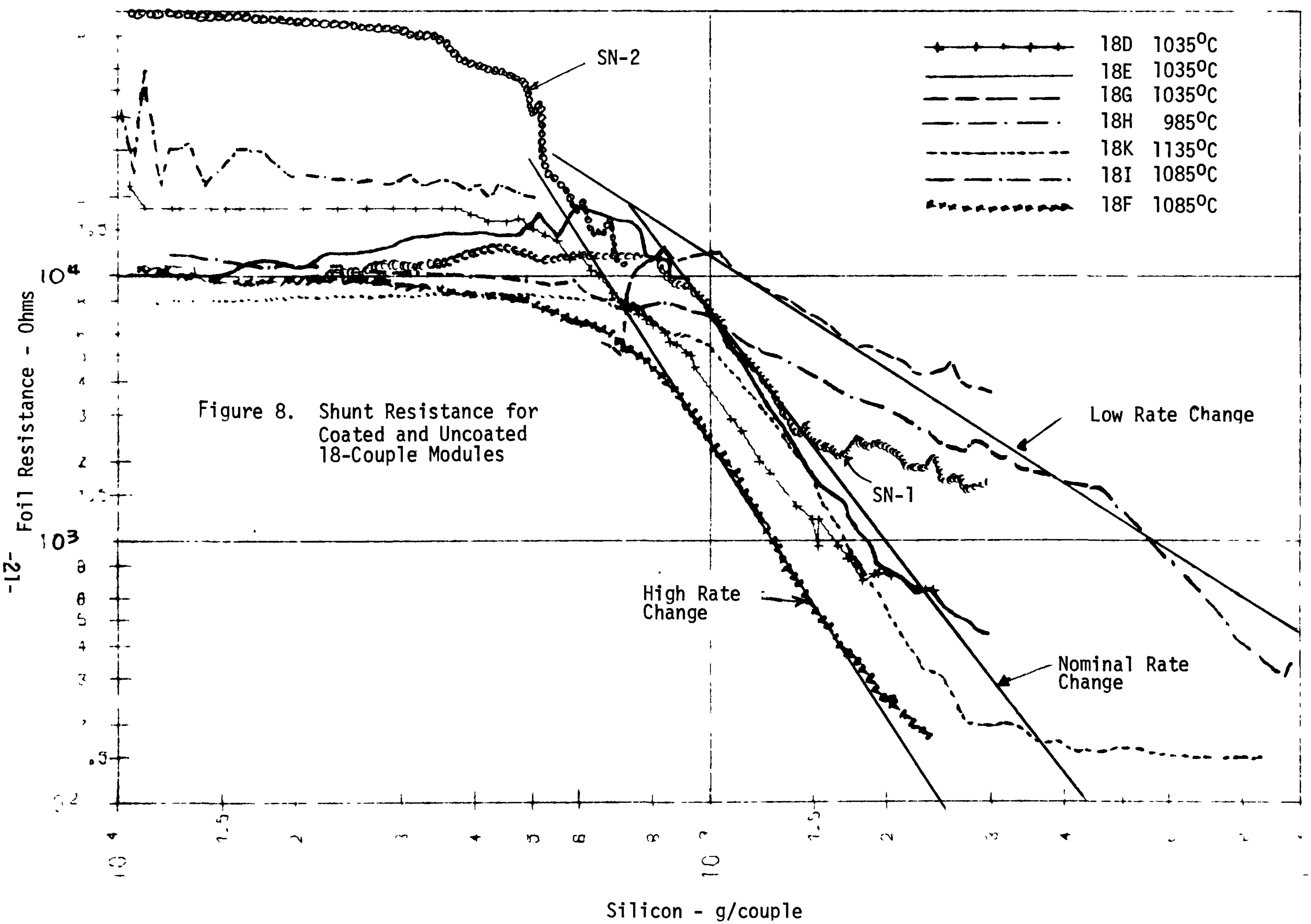

Figure 8. Shunt Resistance for Coated and Uncoated 18-Couple Modules

900-755

SECTION VII

DEGRADATION DUE TO THERMAL INSULATION CHANGES

The same reaction products (SiO) which were responsible for a decrease in the electrical shunt resistance are also the cause of the change in the insulation's thermal conductance. This change in the thermal conductance manifests itself in an increased heat loss through the thermal insulation. Any increased heat flowing through the thermal insulation will correspond to a decrease in the heat flowing through the thermopile, thus reducing the amount of available output power. Again, the 18-couple module experiments served as a data base from which the rates at which these changes take place are calculated. A computer program was developed at JPL for the reduction of the 18-couple module data (Ref. 6). This program was recently modified to account for the change in the SiGe thermoelectric material thermal conductivity (described in a previous section above). Using the heat balance equation, the amount of heat which flows through the thermal insulation package is calculated for each data point, and its rate of change (normalized conductance) is plotted as a function of the effective silicon source (also previously described). Figure 9 shows this change in insulation conductivity for the uncoated 18-couple module, while Figure 10 shows the same data, but for the modules which utilize the protective Si_3N_4 coating. Again, some spread in the data is apparent; however, an envelope encompassing the lowest rate of change and the highest rate of change which can be expected is shown in Figure 11. This figure also shows a nominal (most likely) rate of change. Equations describing all three rates have been developed and are utilized in the DEGRA code to evaluate the total range of possible degradation rates.

Figure 9. Insulation Thermal Conductivity Changes for Uncoated 18-Couple Modules

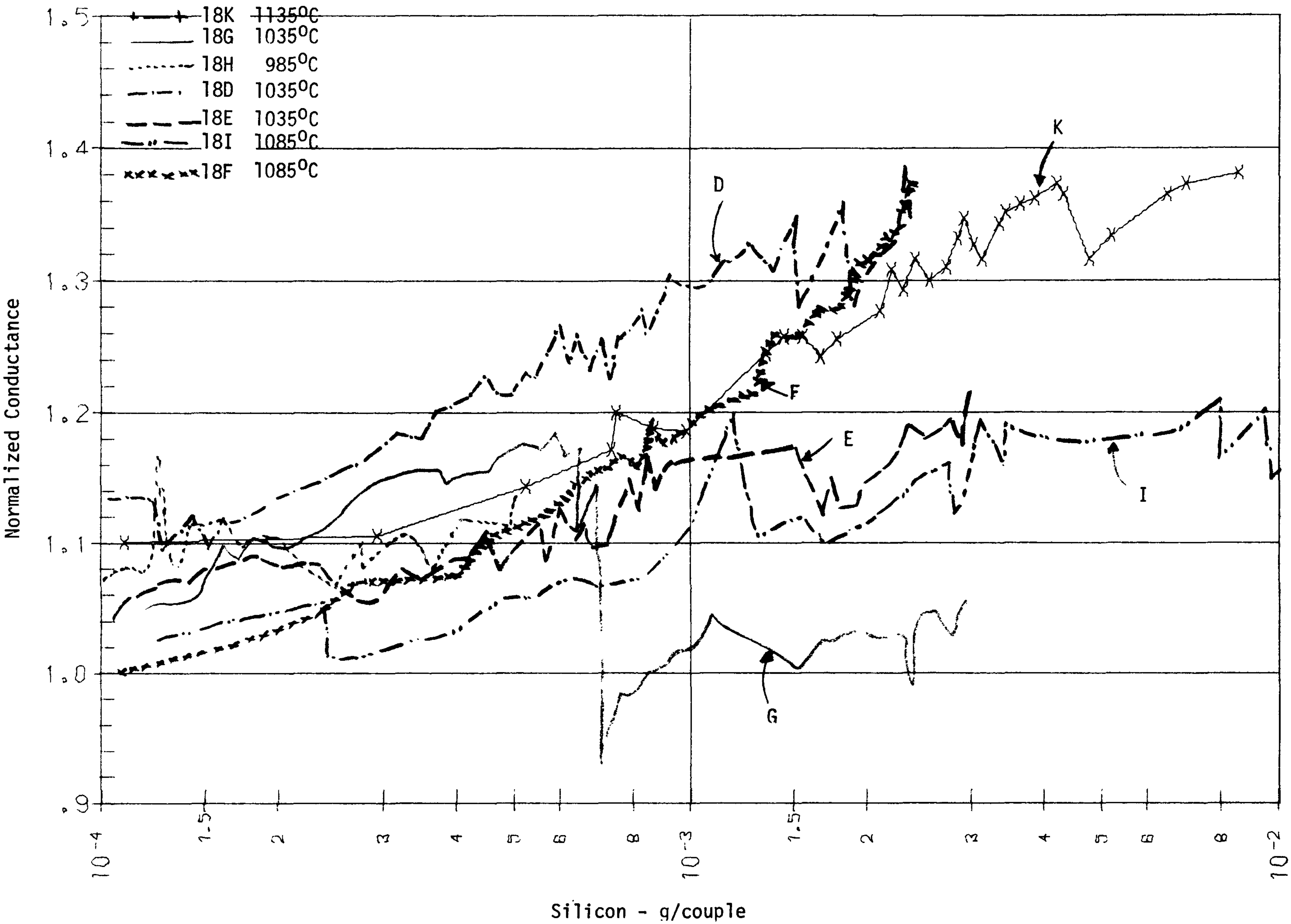

Figure 10. Insulation Thermal Conductivity Changes for Si_3N_4 Coated 18-Couple Modules

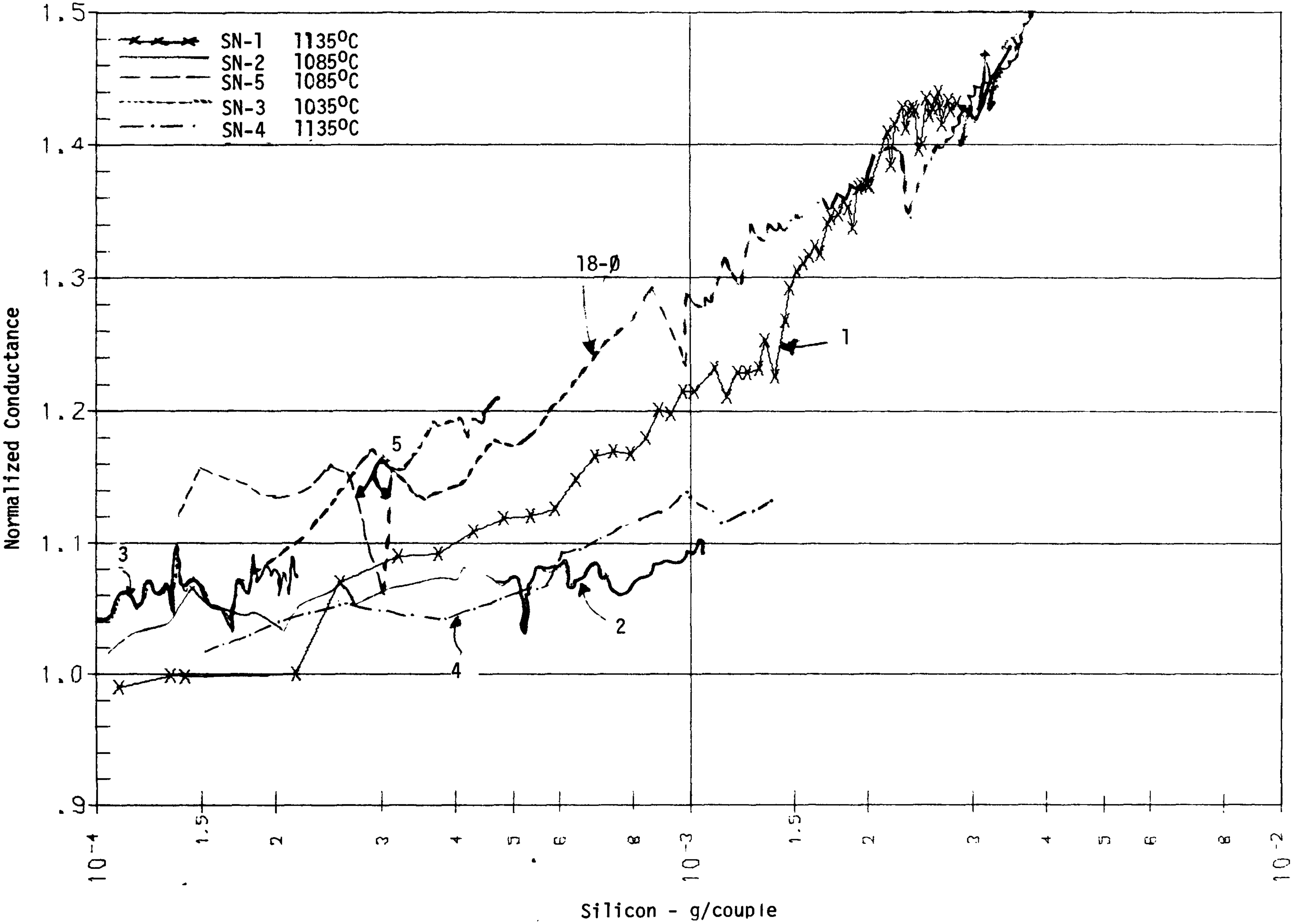

900-755

K+E SEMI-LOGARITHMIC 359-81
KEUFFEL & ESSER CO. MADE IN U.S.A.
4 CYCLES X 70 DIVISIONS

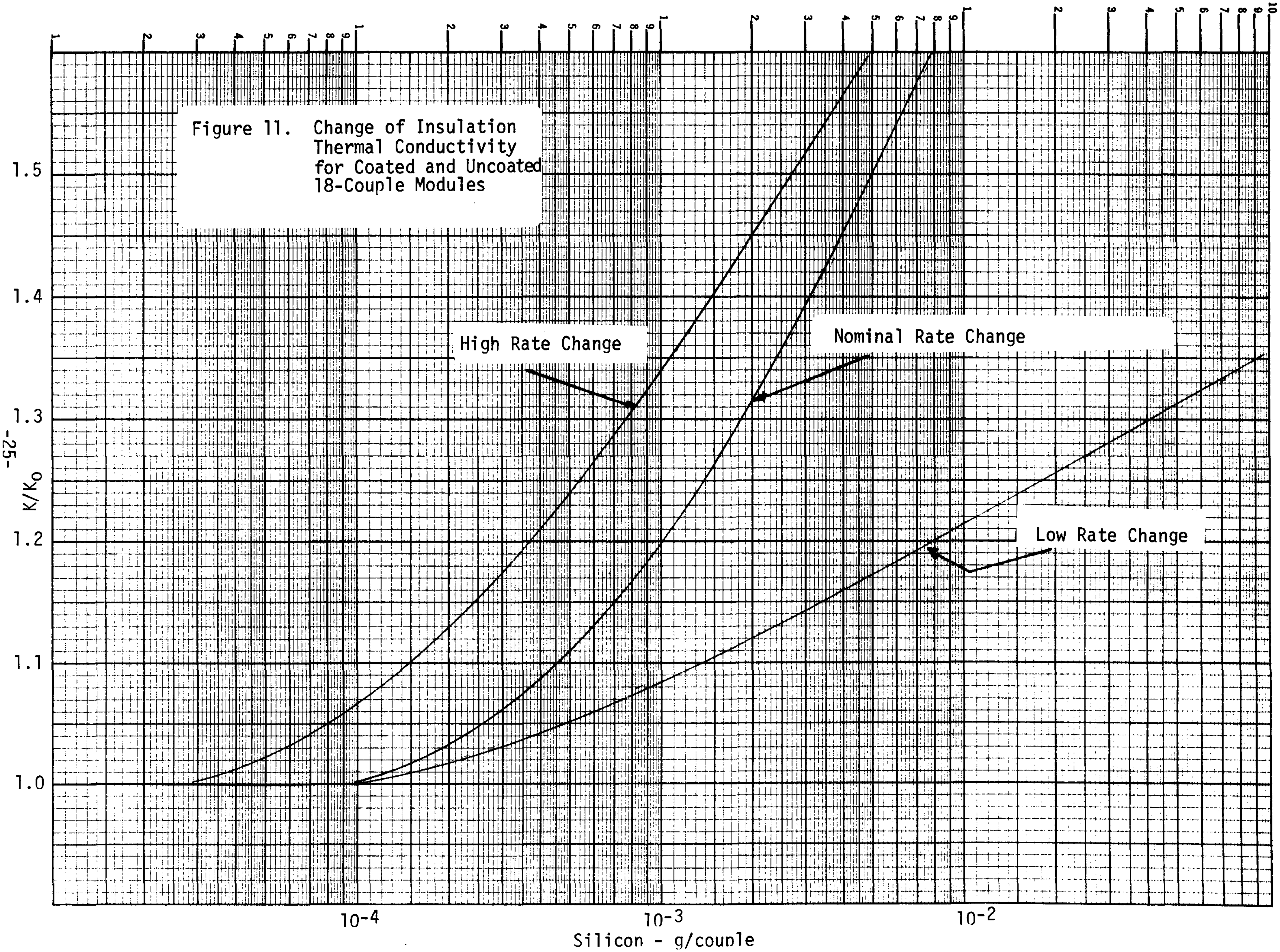

Figure 11. Change of Insulation Thermal Conductivity for Coated and Uncoated 18-Couple Modules

900-755

SECTION VIII

SILICON NITRIDE COATINGS AND THEIR LONGEVITY

To reduce the amount of sublimation from the hot shoe and the unicouple legs which can react with the thermal insulation, the unicouples were coated with a thin layer (nominal 12,000 Å) of Si_3N_4. This Si_3N_4 coating was extensively evaluated at JPL and was found to afford a reduction in the sublimation rate by an order of magnitude. Si_3N_4 coated hot shoe and SiGe samples were placed on test, isothermally, at various temperatures. The samples were then periodically weighed and weight loss rates computed as a function of time and temperature. Similar experiments were conducted in an environment of carbon monoxide (CO) at pressures of 1×10^{-4} Torr. The purpose of the CO testing became necessary when it was determined that a continuous generation of CO takes place within the generator (see below). These coupon experiments not only yielded information on the loss rate of the Si_3N_4 coated material, but also allowed a prediction as to lifetime of the coating. Both the operating temperature and the CO pressure determine the coating longevity, however, sufficient data are only available as a function of operating temperature since the CO experiments have only been performed at the one pressure level (1×10^{-4} Torr). A preliminary estimate as to the Si_3N_4 coating lifetime has been made based on the presently available data and is shown in Figure 12 for three different hot shoe temperatures and as a function of CO pressure. The curves were generated by plotting the two points (at each temperature) which were obtained from actual experiments (i.e., the 10^{-4} Torr point and vacuum point) and connecting them with a straight line. Note that the vacuum data were plotted at 10^{-7} Torr of CO. At this pressure, the effects observed at 10^{-7} Torr due to CO interaction should be only 1/1000 of the 10^{-4} Torr effect and thus be negligible. In reality, it would be expected that the curve connecting the 10^{-4} Torr and 10^{-7} Torr points should be concave downward (i.e., the lifetime would approach the vacuum lifetime in an asymptotic fashion). Therefore, the straight line would give a conservative estimate of the coating lifetime (i.e., lower lifetime). The three temperatures in Figure 12 were chosen to indicate the nominal hot junction temperature (1000^{o}C), the maximum temperature at which 18-couple modules are operated (1100^{o}C), and the maximum off-design temperature (1015^{o}C) which would occur if the MHW isotope fuel loading were increased by 40 thermal watts. This latter case is discussed in more detail later.

The CO pressure within the RTG depends upon the amount of CO generated as well as the conductance of the CO out of the generator. CO is generated at the high temperature where silicon sublimes from the hot shoes. Figure 13 shows the hot shoe and surrounding region of a typical unicouple. Three separate regions have been defined, based on their respective probability of producing SiO. These regions are designated S_1, S_2 and S_3 in Figure 13.

All of the silicon which evolves from the top of the hot shoe (area S_1) can be assumed to react with the graphite:

$$Si + C \rightarrow SiC$$

and thus will not generate any CO. Half of the silicon which comes from the side of the hot shoe (area S_2) will also react with the graphite thus forming SiC, while the other half reacts with the SiO_2 cloth:

$$Si + SiO_2 \rightarrow 2\ SiO$$

This SiO gas can react with the heat source:

$$SiO + 2C \rightarrow SiC + CO$$

thus producing CO. Since the conductance for the SiO gas is very much larger

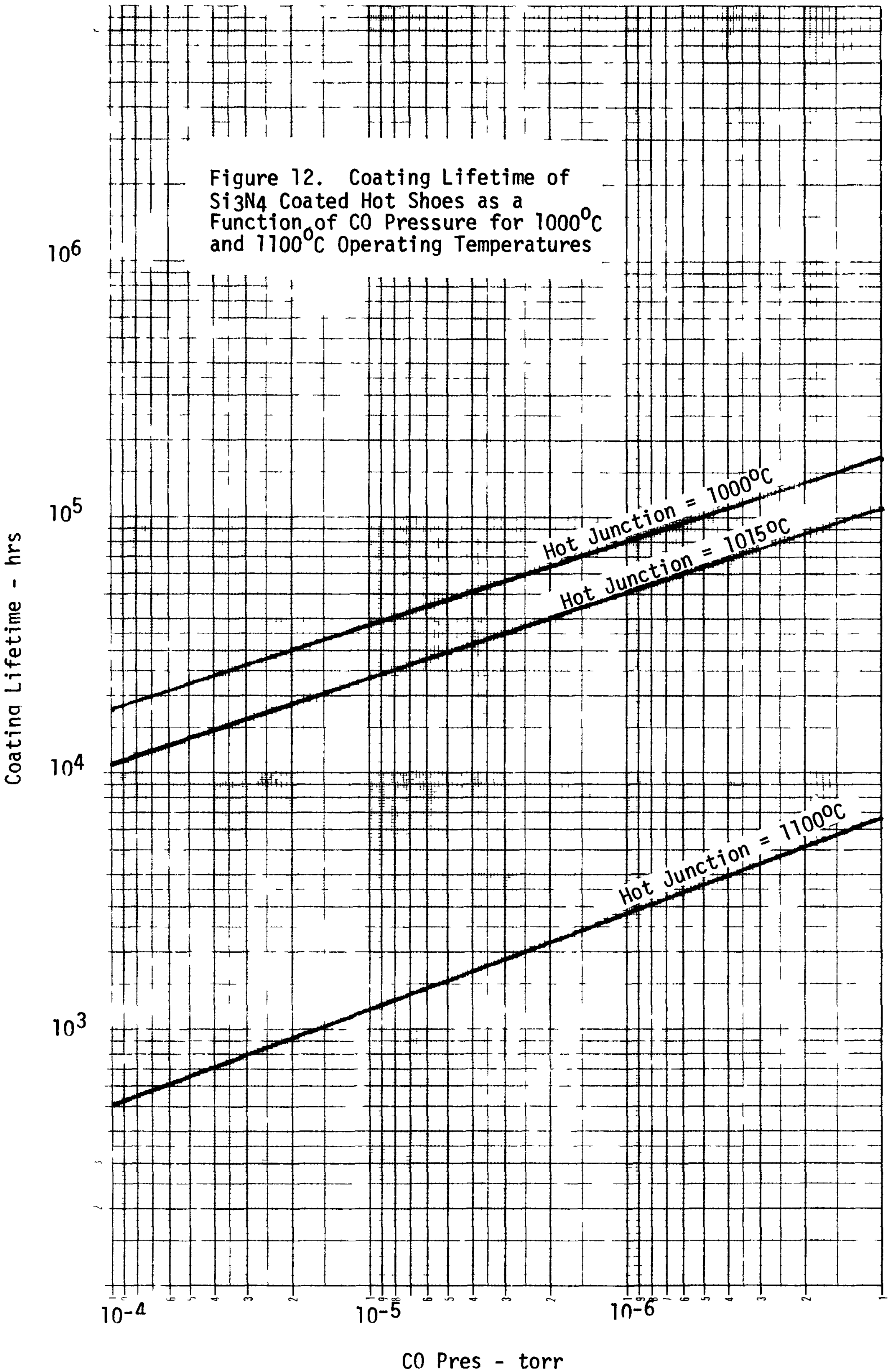
Figure 12. Coating Lifetime of Si3N4 Coated Hot Shoes as a Function of CO Pressure for 1000°C and 1100°C Operating Temperatures
Coating Lifetime - hrs
10^6
10^5
10^4
10^3
Hot Junction = 1000°C
Hot Junction = 1015°C
Hot Junction = 1100°C
10^-4
10^-5
10^-6
CO Pres - torr

Figure 13. The MHW Unicouple and Surrounding Hot Shoe Area

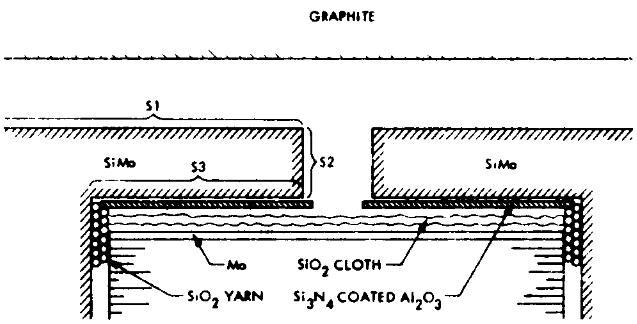

in the direction of the heat source (i.e., between two hot shoes) than it is toward the leg of the unicouple (behind the individual hot shoe), it can be assumed that all of the SiO generated will react with the graphite to produce a continuing source of CO. The silicon which could potentially evolve from the third area (S_3) is assumed to be baffled by the Al_2O_3 spacer and does not contribute to the silicon source or to CO generation.

The amount of sublimed silicon which reacts in such a way as to eventually form CO is thus only dependent upon the area and temperature of S_2. For the multihundred watt (MHW) unicouple, S_2 is found to be 1.6 cm^2 per unicouple, and since only half of the silicon will have a chance to produce SiO, the effective area (A_{eff}) is 0.8 cm^2 per couple. The amount of CO which is generated in the MHW-RTG is thus

$$S = A_{eff} \times R \times \text{No. Couples} \times 2^*$$

where S = CO generated in g/generator-hr

A_{eff} = effective area contributing to SiO reaction in cm^2

R = rate of silicon loss (depends on temperature) in g/cm^2-hr

* the factor of two is required because every Si atom produces 2 CO molecules

At a hot shoe temperature of 1035^oC, an MHW-RTG with Si_3N_4 coated unicouples will produce the following amount of CO:

$$S = 0.8 \times 6 \times 10^{-8} \times 312 \times 2$$

$$S = 3 \times 10^{-5} \text{ g/gen-hr}$$

$$S = 8.32 \times 10^{-9} \text{ g/gen-sec}$$

To make an estimate of the CO pressure within the MHW-RTG, the conductance of CO out of the generator must be known under equilibrium conditions. The sum of all leakage and reaction rates must balance the generation rate. Based on Reference 7, the reaction of CO in the hot shoe region does not constitute a sink for CO and therefore does not need to be considered. (It was shown in Reference 7 that every molecule of CO that reacts with the hot shoe will eventually result in another molecule of CO.) Thus, at equilibrium, the CO generation rate will equal the rate at which leakage takes place.

The three primary leakage paths out of the generator are shown in Figure 14. The values of conductance for the hole in the foil basket and the PRD valve are based on Reference 8. The unicouple leg conductance is based on experiments performed at JPL using a single unicouple. All of the conductances are at room temperature and for gases having a molecular weight of 28 (N_2 or CO). The conductance at the appropriate operating temperatures are shown in parenthesis. It can be seen from the figure that the total conductance of the generator will be primarily governed by the PRD conductance value. The mass flow rate can be calculated based on this total conductance as a function of CO pressure. Figure 15 shows this rate for the MJS MHW generator using a total conductance value of 1.99 l/s. Also shown in the figure is the CO generation rate for the same generator. The intersection of the two lines represents the equilibrium pressure of the system, which can be seen to be somewhat below the 1×10^{-5} Torr pressure level (8×10^{-6} Torr).

Different systems will, of course, have different CO pressures. Figure 16 shows the probable CO equilibrium pressure for typical 18-couple modules operating at three different hot shoe temperatures, thus three rates of CO generation. For these modules, two different conductances are shown, e.g., a maximum conductance and a minimum conductance. These values of conductance are based on experiments performed at JPL on single unicouples, and the maximum and minimum values represent the range of results obtained. It is assumed that the total conductance of each module is due only to the 18 penetrations caused by the unicouples inserted into the surrounding foil basket. This may be more inaccurate in the case of the 18-couple modules than in the case of the MHW-RTG since

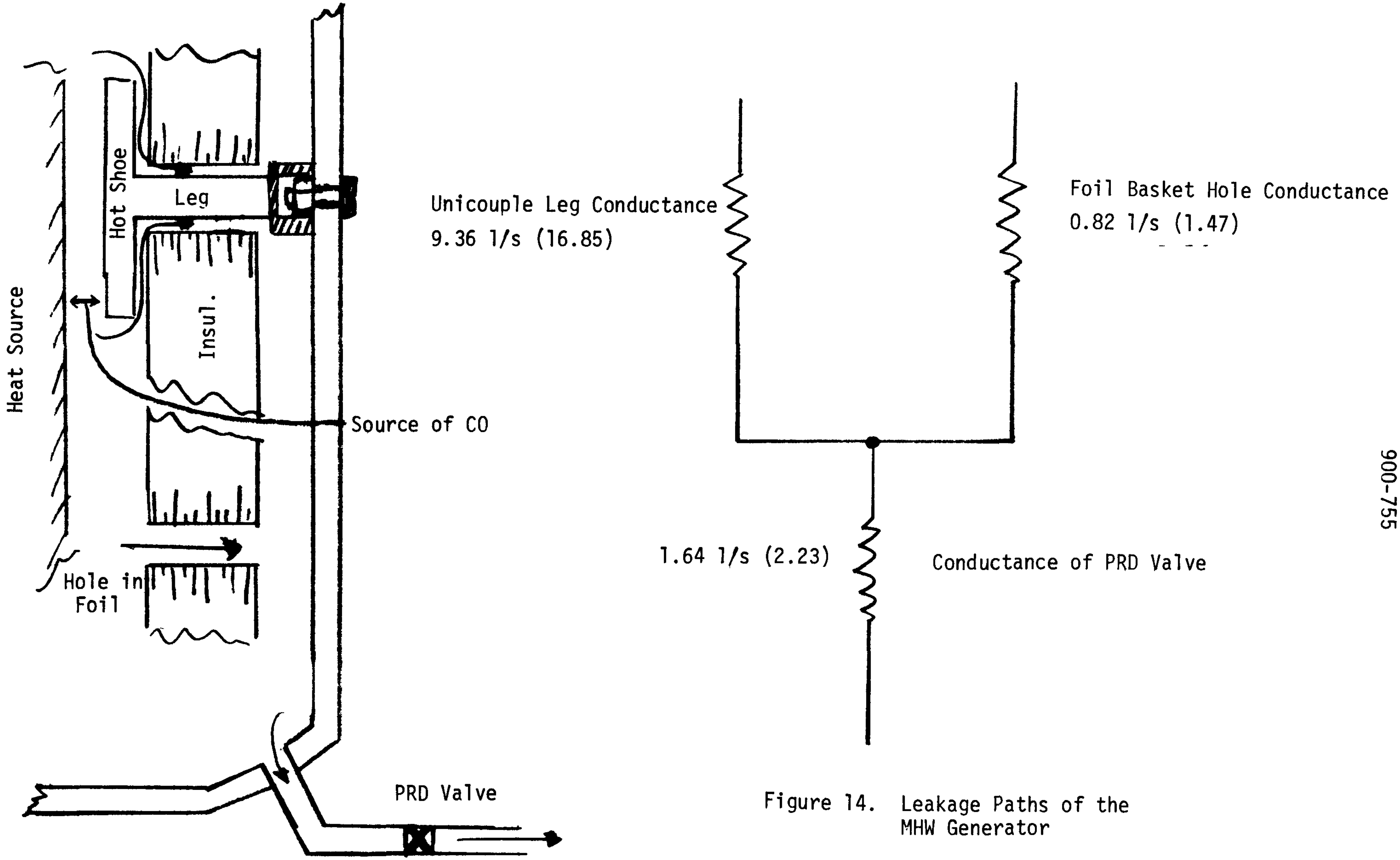

Figure 14. Leakage Paths of the MHW Generator

900-755

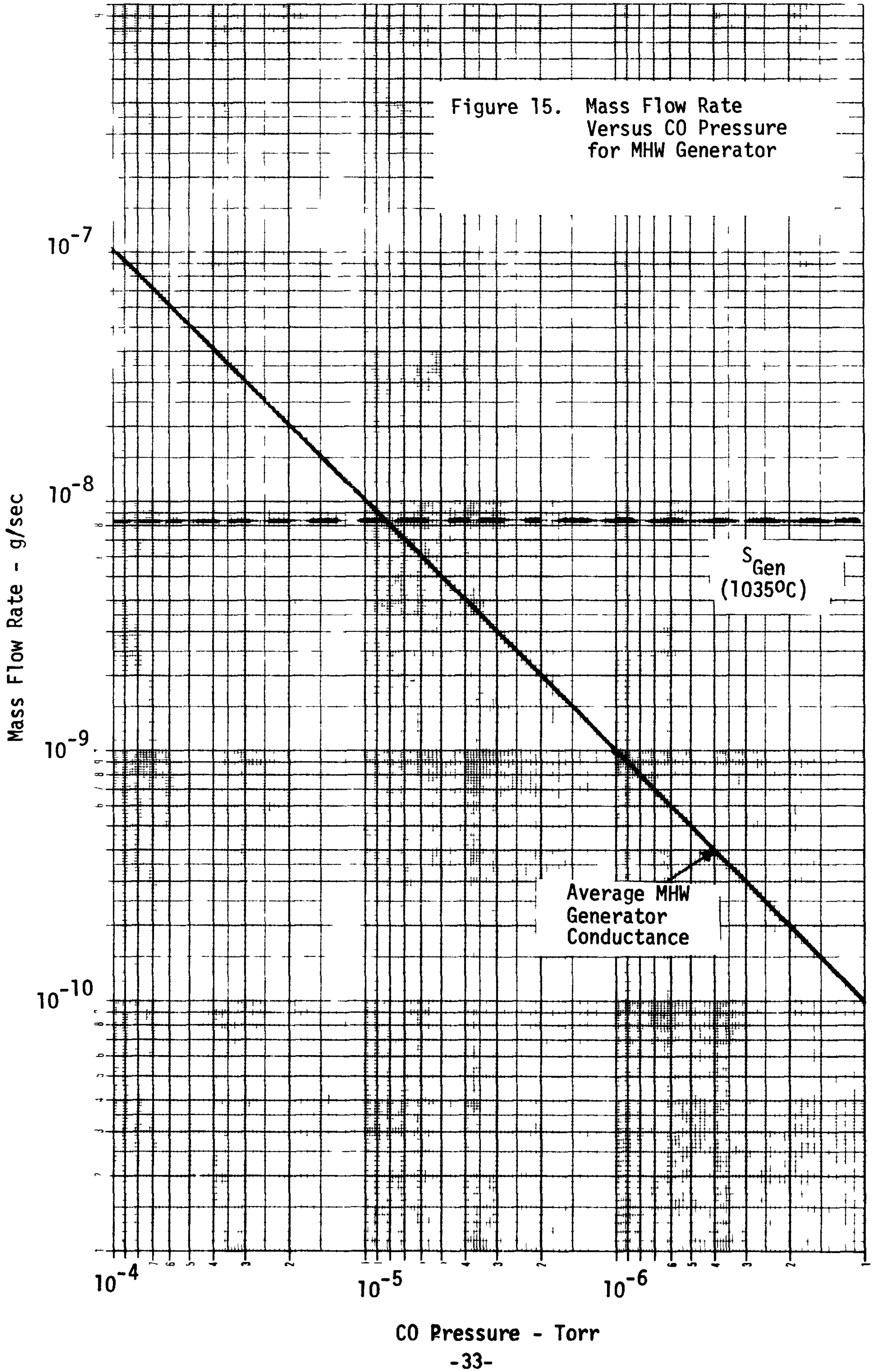
Figure 15. Mass Flow Rate
Versus CO Pressure
for MHW Generator
10^{-7}
10^{-8}
10^{-9}
10^{-10}
Mass Flow Rate - g/sec
S_{Gen}
(1035°C)
Average MHW
Generator
Conductance
10^{-4}
10^{-5}
10^{-6}
CO Pressure - Torr

the module may have larger conduction passages along the edges of the foil basket than would a full-up RTG. Thus, the values should represent minimum conductances. Note also that the 18-couple module has no PRD valve. (The PRD valve, it will be recalled, was the major constriction in the MHW system.) Therefore, the total conduction path is based solely on 18 parallel unicouple penetrations. Based on the experiments at JPL, the conductance per couple was found to be 0.02 ℓ/s to 0.04 ℓ/s (at room temperature). The data in Figure 16 show that only the modules operating at the elevated temperatures (1135^{o}C) will operate at comparable CO pressures as is expected for the complete generator (near 1 x 10^{-5} Torr level), while all of the lower temperature modules will operate in a CO environment which is considerably less severe than that of the generator.

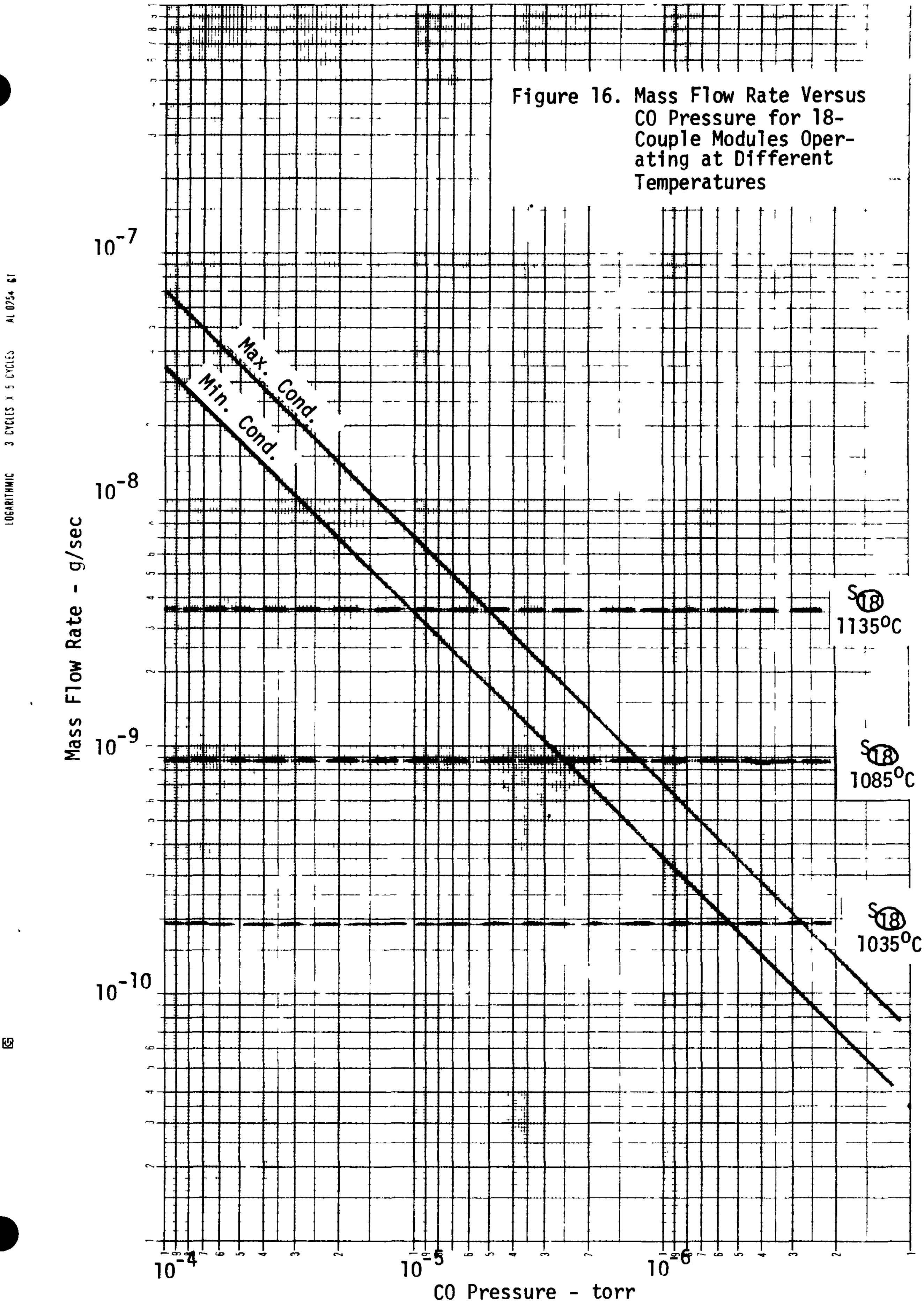

Figure 16. Mass Flow Rate Versus CO Pressure for 18-Couple Modules Operating at Different Temperatures

SECTION IX

VERIFICATION OF THE DEGRA CODE

Since the stated objective of the DEGRA computer code is to predict the available output power of an RTG at any given time, its usefulness will be reflected by the confidence which can be placed in its accuracy. Considerable effort has therefore been made in comparing the results of the computer program with data which is available from experiments. The largest body of data for this verification is probably represented by the 18-couple modules which have operated for extended periods of time and at various temperatures. To accomplish this, the DEGRA code was modified slightly to represent an 18-couple module rather than an MHW generator. Several parameters can be compared on a direct basis between the actual measured values and the values predicted by DEGRA.

The comparison of some of these parameters is shown in the following figures. Figure 17 compares the change in internal resistance as a function of time for three 18-couple modules which operate at 1135^{o}C with that predicted by the DEGRA code. The data shows very close correlation between experiments and predictions. Since this parameter is least sensitive to temperature, the best agreement would be expected. The Seebeck coefficient, which is very sensitive to temperature, nevertheless indicates good agreement as can be seen in Figure 18, which compares the same 18-couple modules with the DEGRA code.

Another parameter measured on the 18-couple module is the shunt resistance; the electrical resistance between the unicouples and the thermal insulation. Figure 19 and 20 show this resistance as a function of operating time for SN-1 and 18-0, which operated at 1135^{o}C, and SN-2 and SN-5, which operated at 1085^{o}C. The DEGRA predicted shunt resistance is also shown in both figures. The nominal rate of change is shown to fit the experimental data best at 1135^{o}C operation,

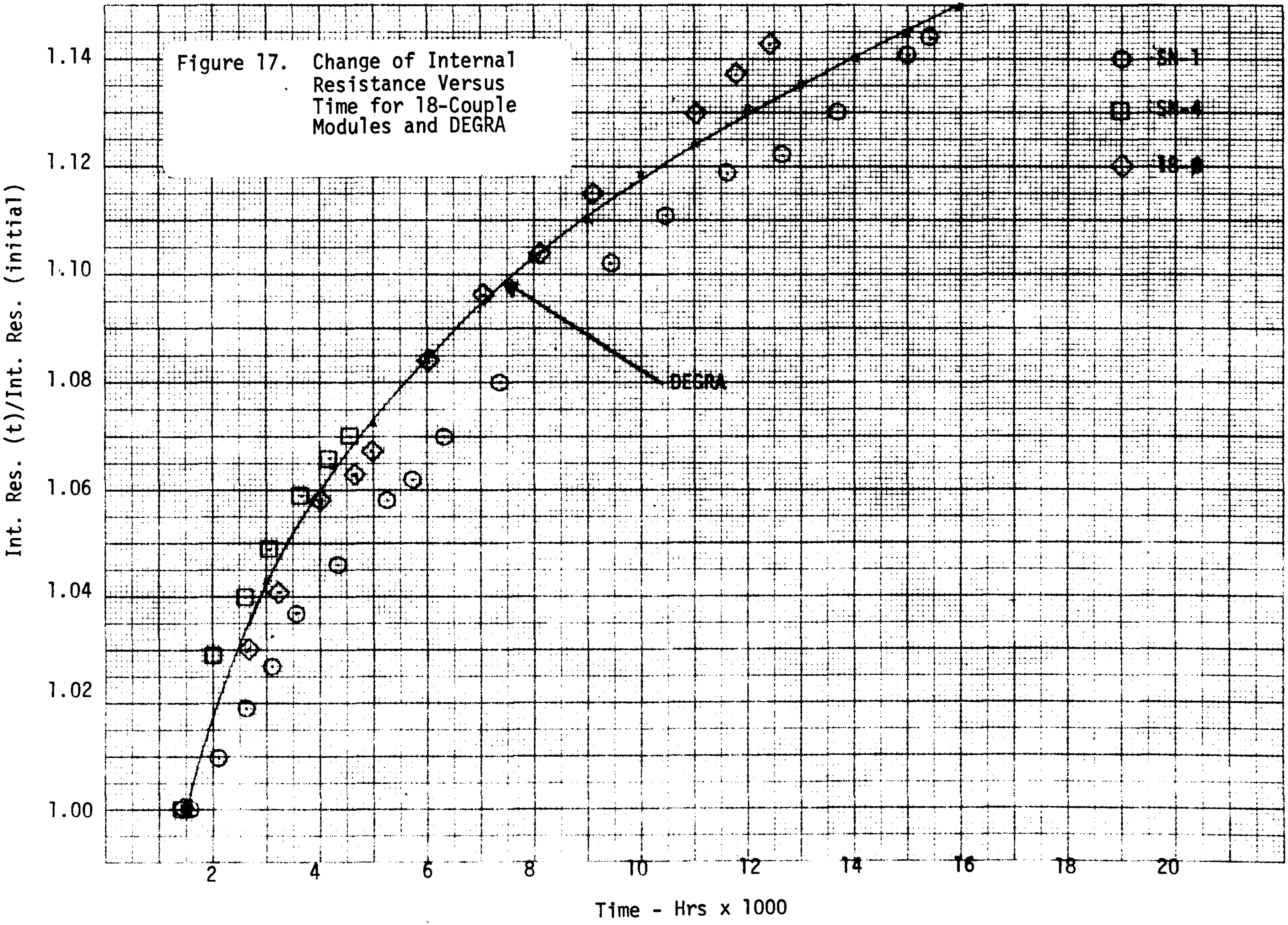

Figure 17. Change of Internal Resistance Versus Time for 18-Couple Modules and DEGRA

900-755

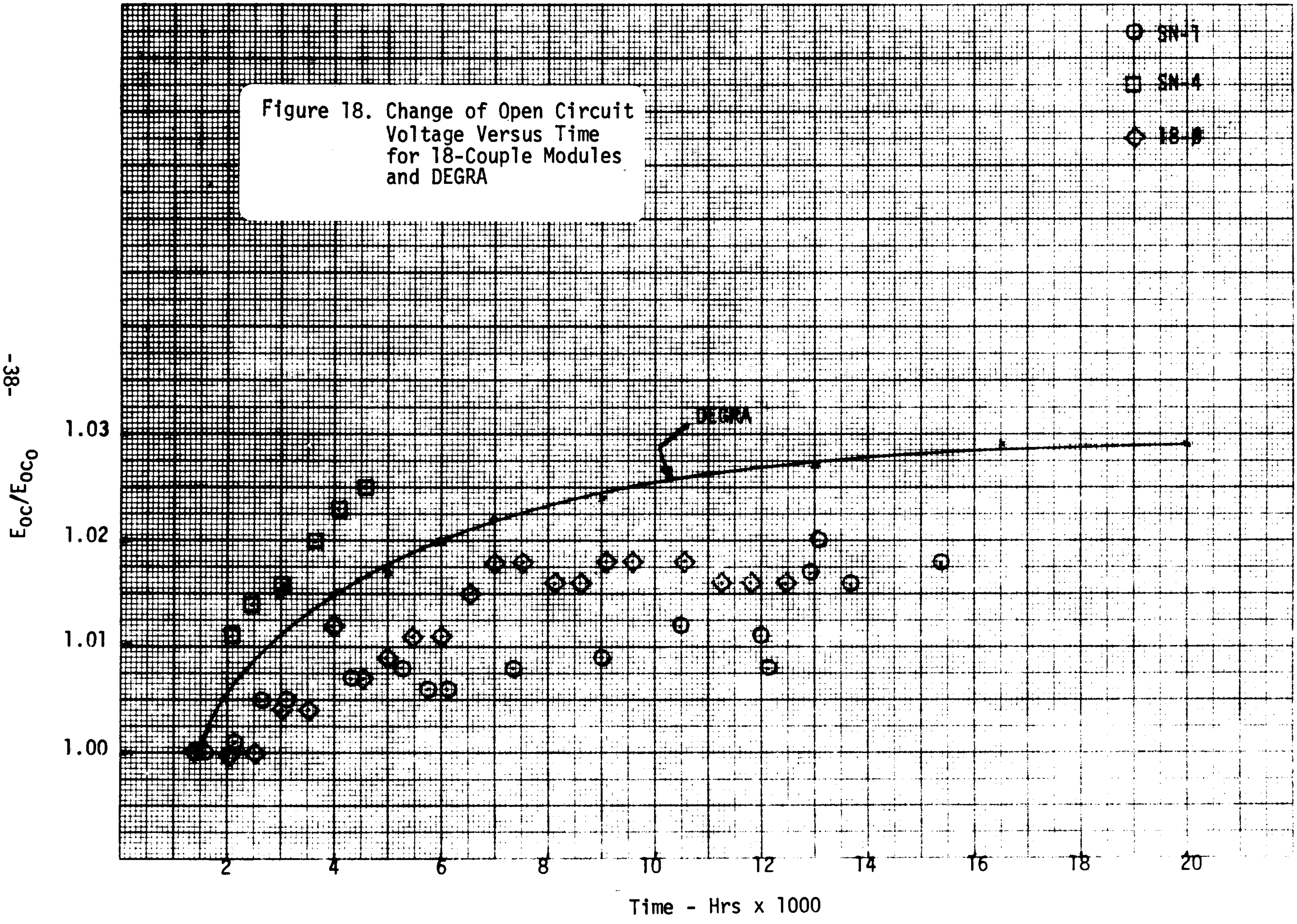

Figure 18. Change of Open Circuit Voltage Versus Time for 18-Couple Modules and DEGRA

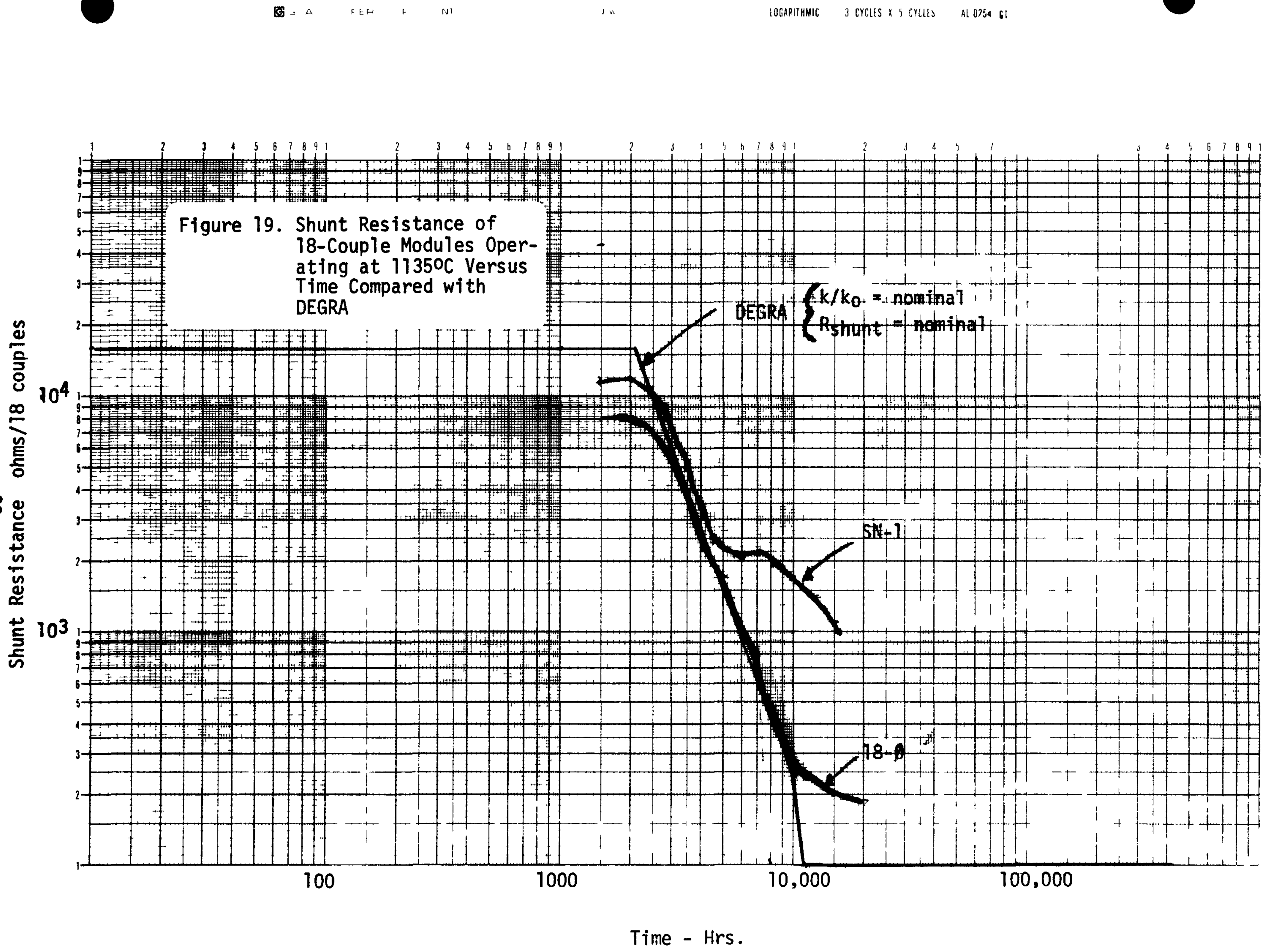

Figure 19. Shunt Resistance of 18-Couple Modules Operating at 1135°C Versus Time Compared with DEGRA

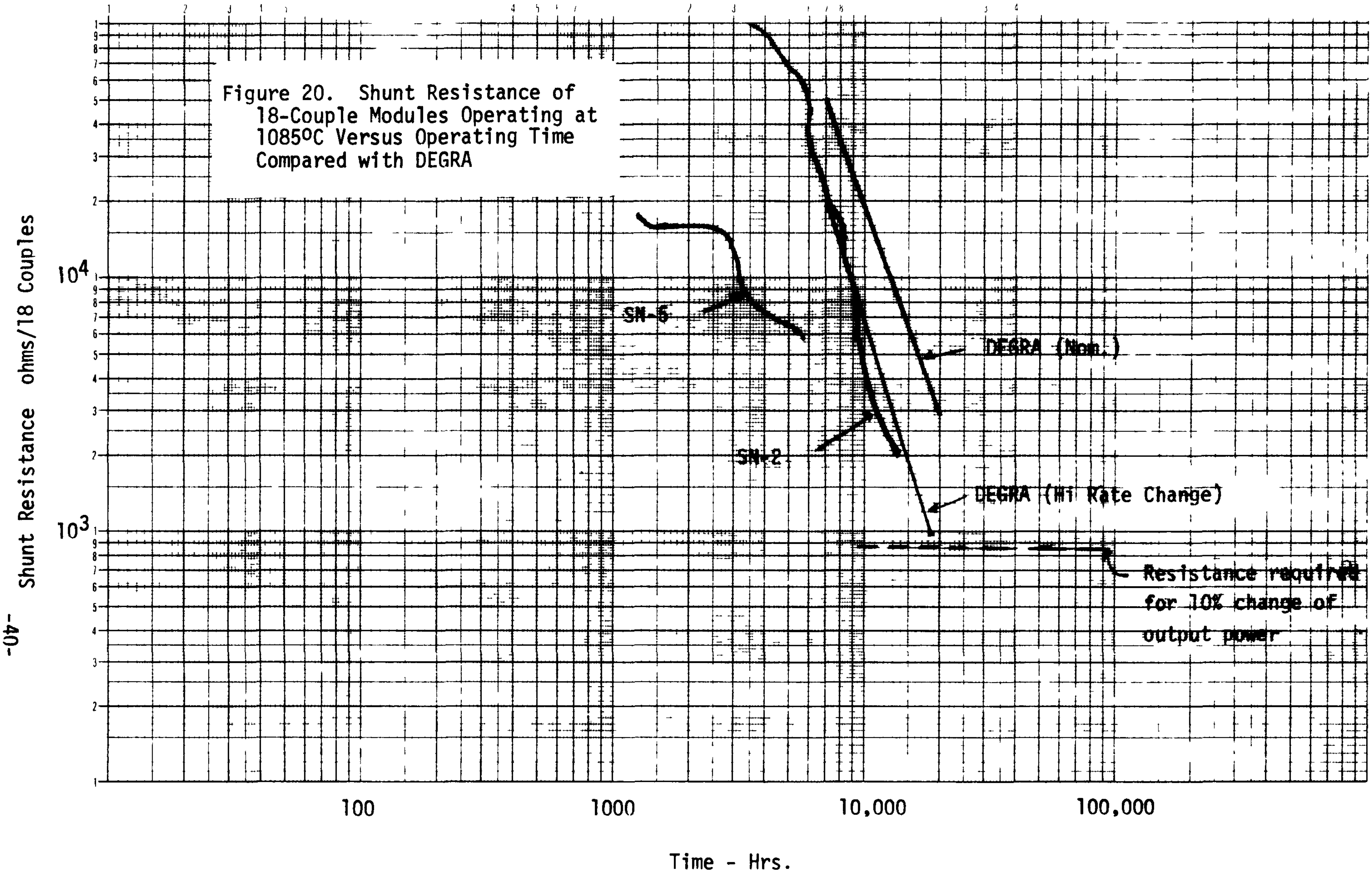

Figure 20. Shunt Resistance of 18-Couple Modules Operating at 1085°C Versus Operating Time Compared with DEGRA

while for SN-2 and SN-5 (1085°C) it appears that the high rate shunt resistance change gives the best fit to the experimental data. Also shown on this graph is the shunt resistance (86.6 ohms/18-couple module, or 5 ohms per generator), which is required to result in a 10% decrease of generator output power. It is more important that the DEGRA code fit the experimental data at the lower shunt resistance rather than at larger values of resistance; remember the higher values have little effect on the available output power.

The all important parameter, the output power, is shown for all of the Si_3N_4 coated 18-couple modules operating at three different hot shoe temperatures (1035°C, 1085°C, 1135°C) and compared with the DEGRA prediction in Figures 21 through 23. The DEGRA data (solid line) follows the experimental data to within 1 - 2% in all cases. At the lower temperatures, the predicted output power is somewhat on the conservative side (lower than actual), while the opposite holds true at the high operating temperatures. It is at this operating temperature (1135°C) that the limited Si_3N_4 coating lifetime will have an effect on the performance. The coating is predicted to be removed somewhere between 1500 and 10,000 hours of operation at this temperature (at least the N-half of the coating, which is the side that has the lowest life expectancy). The large spread is due to uncertainty about the CO pressure and the fact that the temperature decreases with time. The most probable coating lifetime is between 7000 and 10,000 hours. The effect on the output power, which this removal of the coating has, is also shown in the figure (Figure 22), and it can be seen that the experimental data falls somewhere between the fully coated and the partially coated version of the DEGRA prediction.

The prediction shown in Figure 23 for the case where the coating is removed indicates a parallel output power profile (parallel with respect to the completely coated mode) after the initial decrease of output power as the coating comes off. This effect is caused by the use of a limit for the shunt resistance, e.q., the

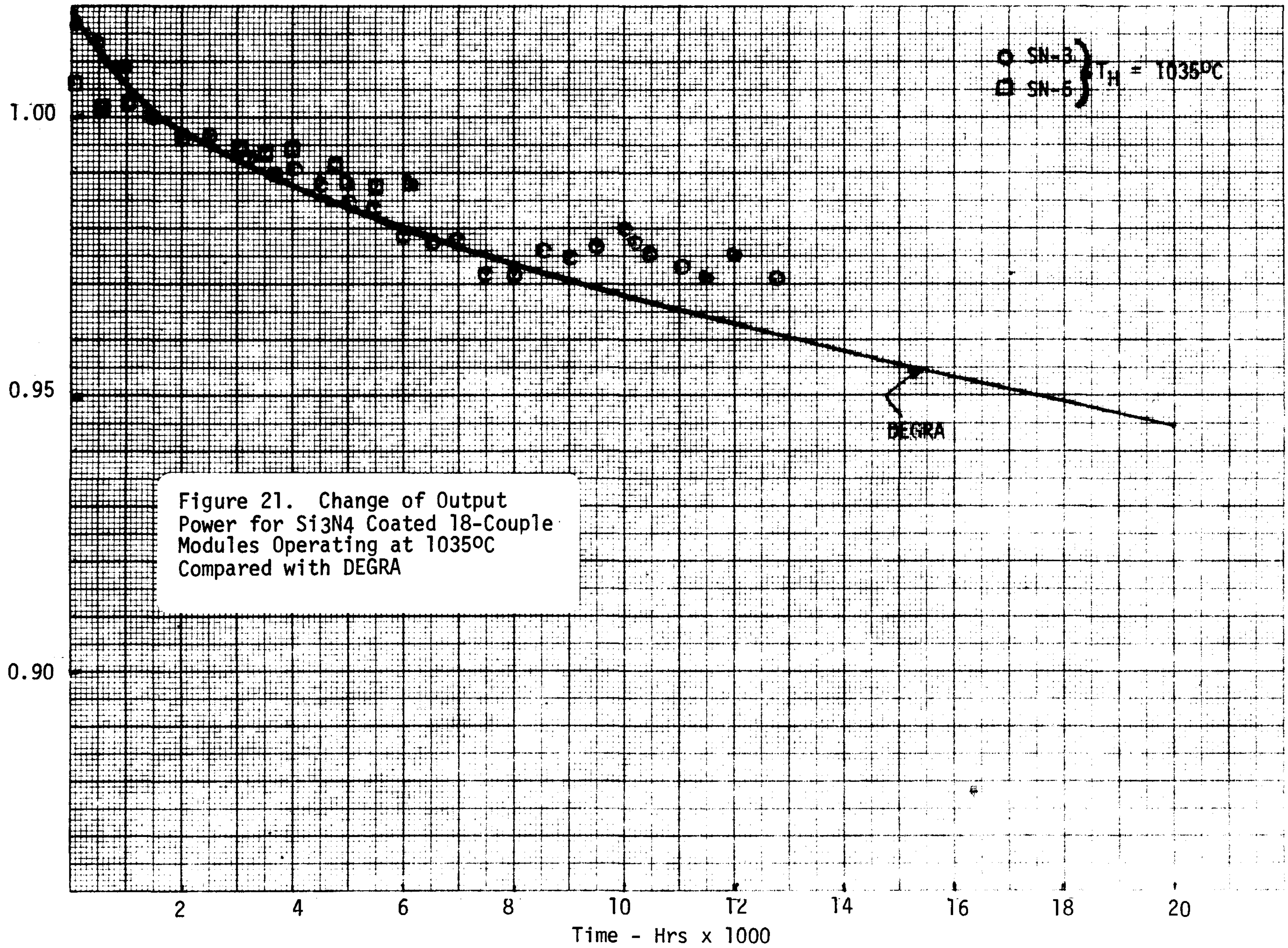

Figure 21. Change of Output Power for Si3N4 Coated 18-Couple Modules Operating at 1035°C Compared with DEGRA

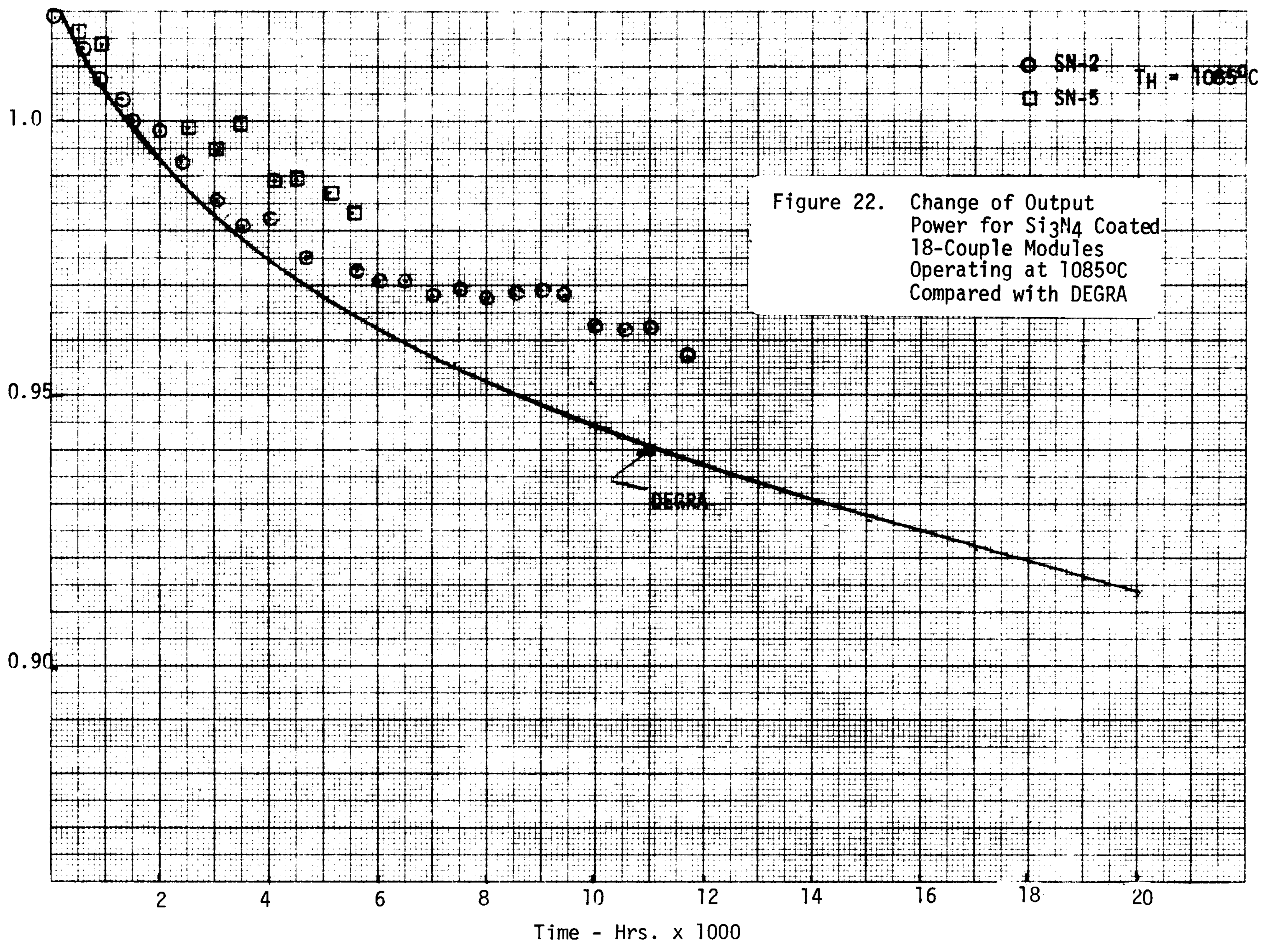

Figure 22. Change of Output Power for Si_3N_4 Coated 18-Couple Modules Operating at 1085°C Compared with DEGRA

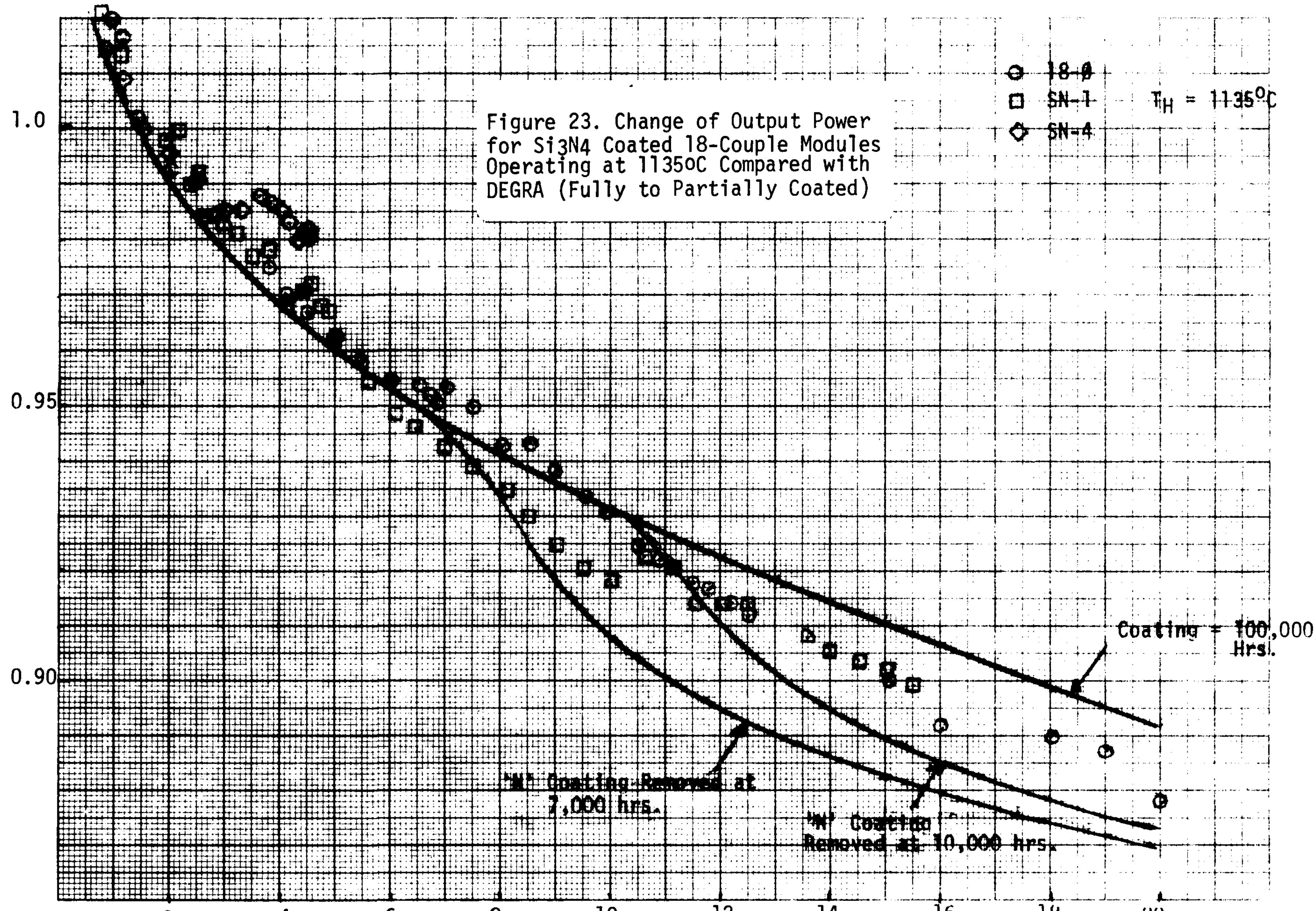

Figure 23. Change of Output Power for Si_3N_4 Coated 18-Couple Modules Operating at 1135°C Compared with DEGRA (Fully to Partially Coated)

900-755

shunt resistance is not allowed to decrease below a predetermined value. This limiting value is based on the 18-couple module data, which shows that the shunt resistance no longer decreases after it reaches a given resistance value. This value lies somewhere between 60 ohms to 100 ohms per 18-couple module (this translates to 3.46 ohms per generator for the case of 60 ohms). The use of this limiting shunt resistance value is important in the prediction of the generator output power, and its effect will be demonstrated in a later section. Sufficient data appears to exist to place the minimum resistance at 60 ohms per 18-couple module.

Only one electrically heated generator (ETG), designated TBC-4, had a sufficiently long operating time to enable comparison with the DEGRA code. Figure 24 shows the shunt resistance of TBC-4 along with the three different shunt resistance rates used in the DEGRA code. Note that the shunt resistance for TBC-4 is shown as a band. The reason for this is that unlike the 18-couple modules, the ETGs have a small temperature gradient along the thermopile axis. Thus the unicouples near the center of the RTG operate at a higher temperature and thus will degrade more rapidly. The hottest unicouples operate about 12°C higher in temperature than the average. The lower end of the range in the TBC resistance data of Figure 24 is obtained by assuming all couples operate at the average temperature. The upper range assumes all unicouples operate at the highest temperature. The most likely curve is one lying between these two curves and favoring the higher temperature curve (to the right-hand side) because of the nonlinear behavior of silicon loss rate versus temperature. Even considering that fact, however, it can be seen that the shunt resistance for TBC-4 is less than the DEGRA nominal and at best matches the DEGRA high rate of change curve. The power output of TBC-4 has also been compared with the DEGRA code. Figure 25 shows this comparison of output power as a function of time. The correlation of the two sets of data is within 0.5%. The nominal rate of change for the thermal

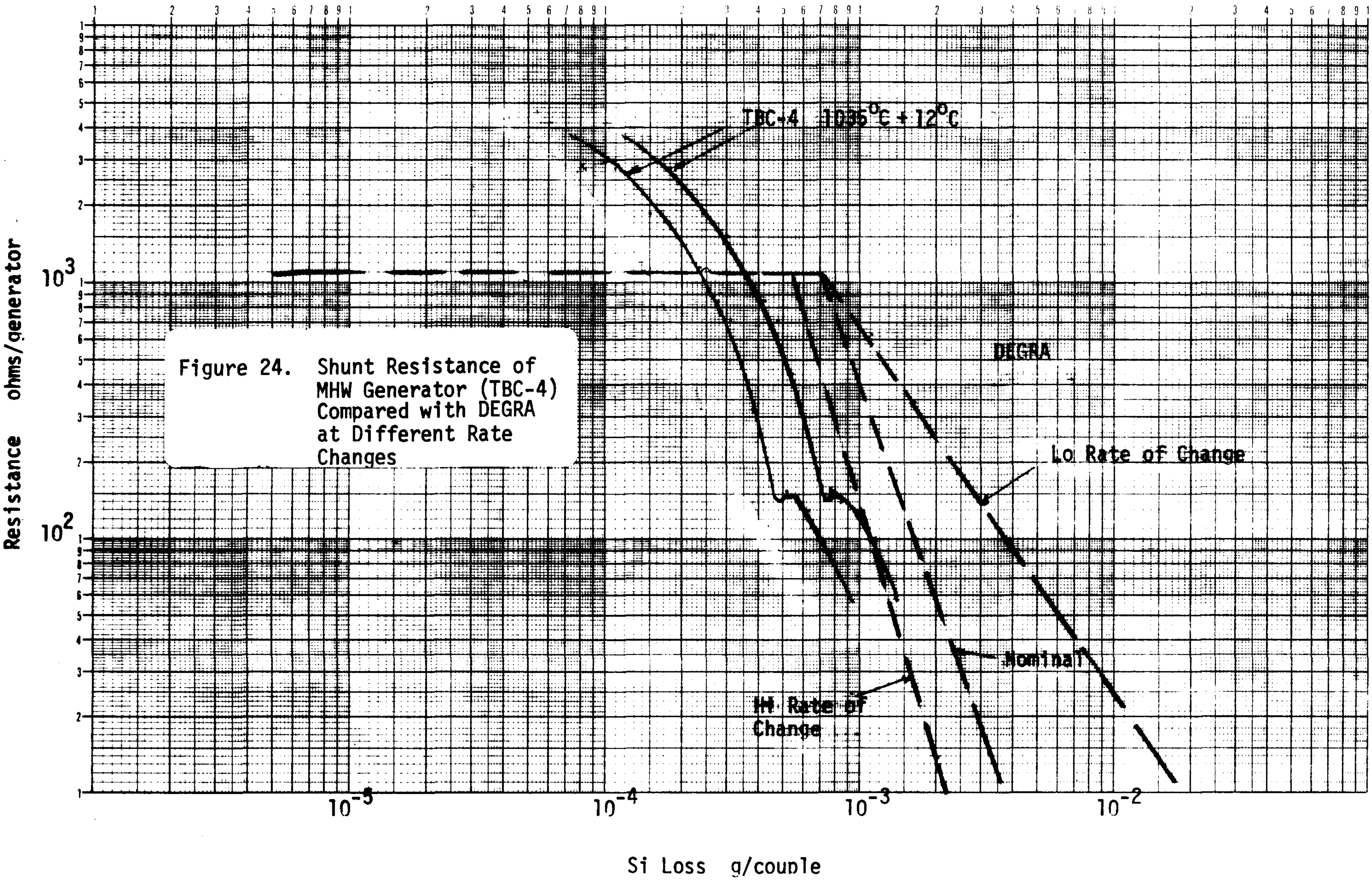

Figure 24. Shunt Resistance of MHW Generator (TBC-4) Compared with DEGRA at Different Rate Changes

900-755

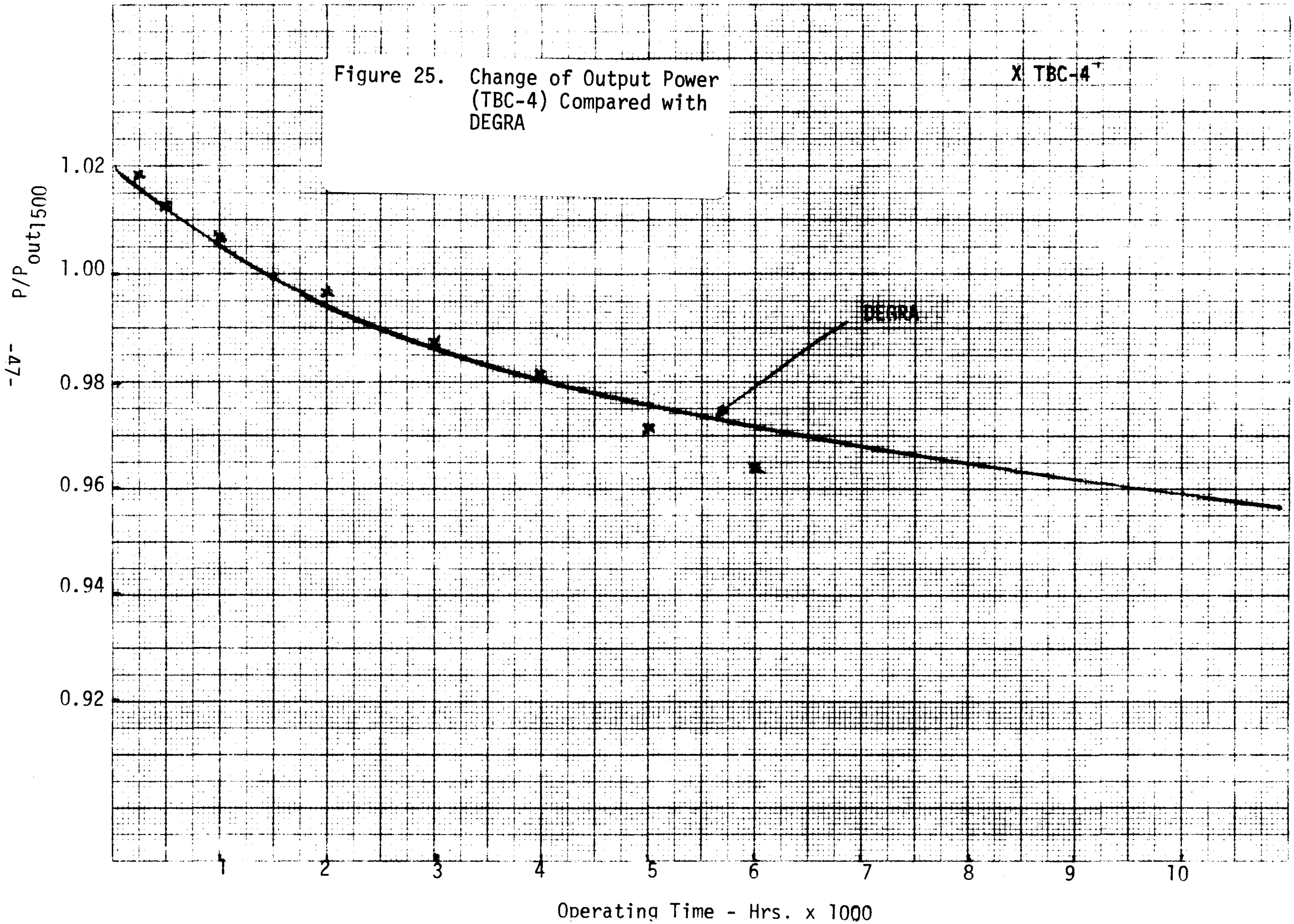

Figure 25. Change of Output Power (TBC-4) Compared with DEGRA

insulation as well as the shunt resistance for the DEGRA code was used for this comparison. The good agreement between the two output power data despite the previously described discrepancy of shunt resistance is not surprising since even at the relatively low generator shunt resistance value (58 ohms), only 1.3 watts (less than 1%) of output power is being lost.

SECTION X

POWER OUTPUT PROJECTIONS FOR THE MHW GENERATOR

The DEGRA code is normalized initially to match the MJS-MHW generator at the 1500 hour point (BOL). All pertinent parameters such as hot and cold junction temperatures, heat leakages, open circuit voltage, internal resistance, output power, etc., are adjusted to match the BOL experimental data of TBC-4. After this initial fine tuning, the code computes the changes of all of the important parameters at discrete incremental time steps to operating times of 90,000 hours. The output power characteristics of the RTG are based on the initial BOL (1500 hour) conditions of a $1000^{o}C$ hot junction temperature, a thermal input power of 2360 watts, and an output power of 155.8 watts.

Figure 26 shows power versus time for the MHW-RTG assuming a coating lifetime greater than 100,000 hours. The effects of maximum and minimum rates of change in the electrical shunt resistance and the insulation thermal conductivity are clearly indicated. The difference in output power is very small since only the thermal conductivity of the insulation affects the available output power, while the shunt resistance remains sufficiently large (as long as coating remains intact) so as not to influence the output power. The effect of Si_3N_4 coating lifetime at the nominal rates of change is shown in Figure 27. Although the coating lifetime has a decided effect upon the available output power, even a complete absence of the coating (uncoated) will not result in a catastrophic failure of the generator under the conditions of nominal rates of change.

The most likely worst case condition would be if the insulation conductivity were to change at the nominal rate, while the shunt resistance changed at the high rate. (The only condition which would be worse, but highly unlikely, would be a low rate of change for the insulation with a high rate of change for the shunt resistance.) Figures 28-30 show this condition for different minimum shunt

Figure 26. DEGRA Output Power for Different Rate Changes (Fully Coated)

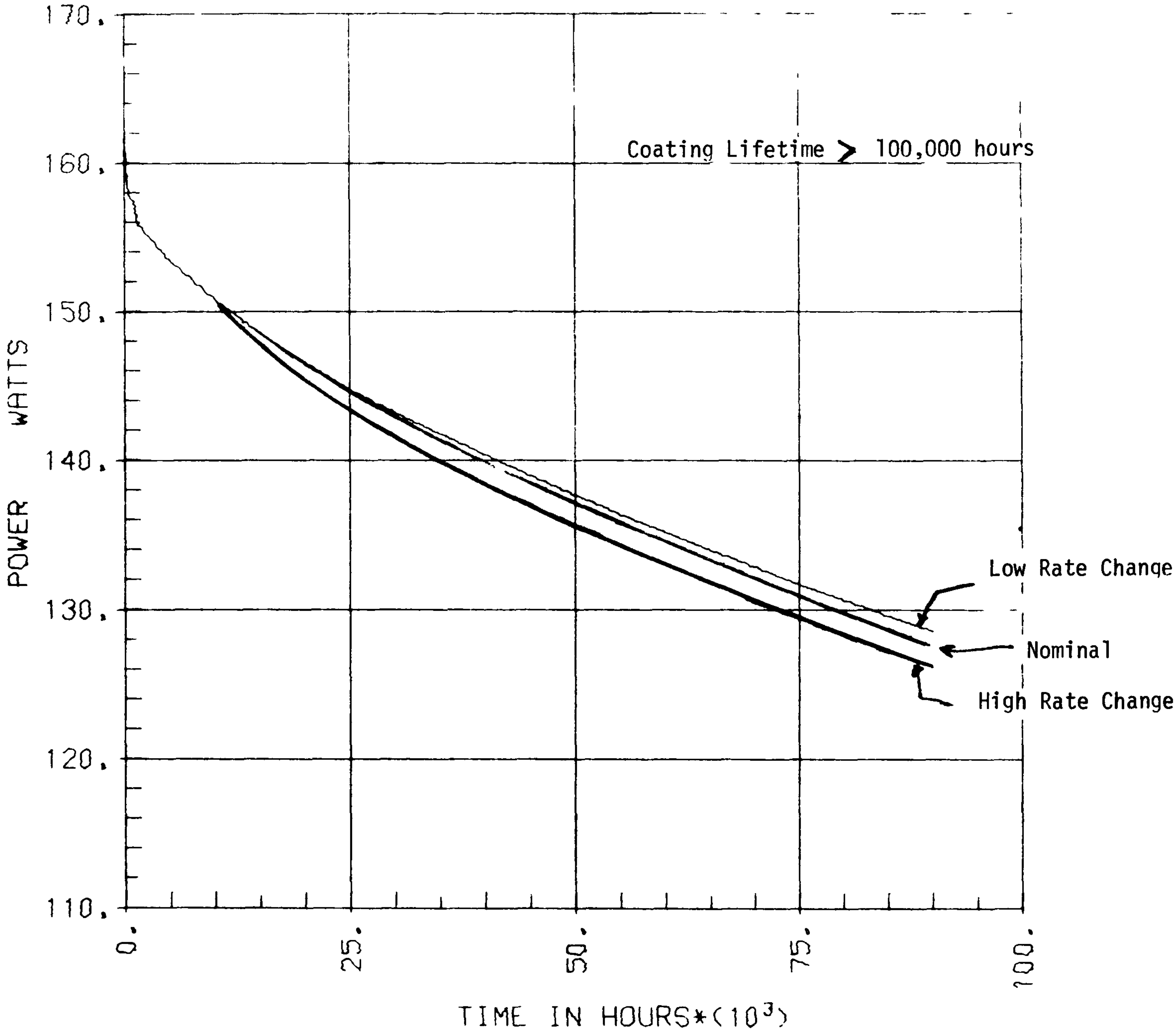

Figure 27. DEGRA Output Power for Nominal Rate Changes and Varying Coating Lifetimes

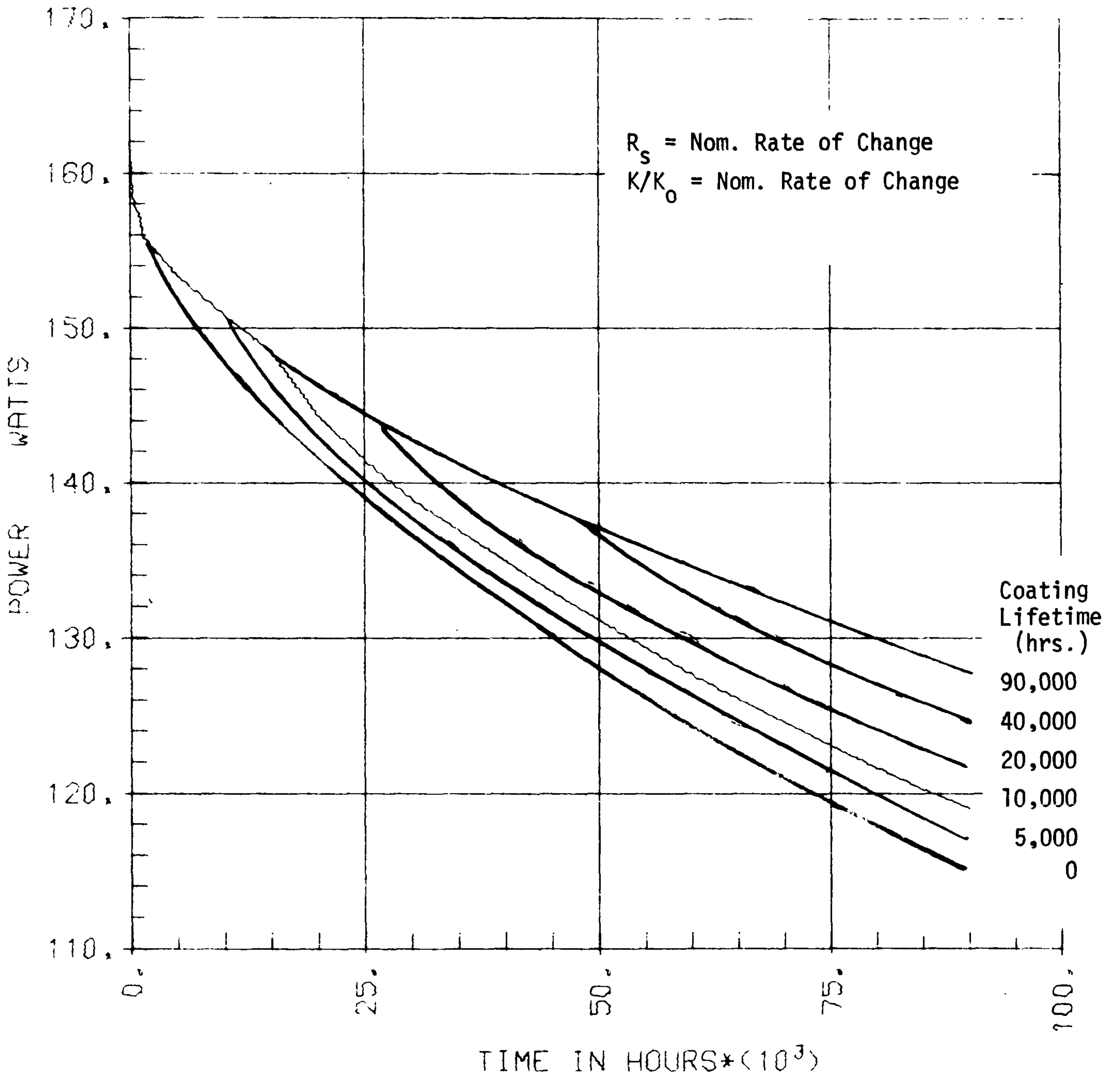

Figure 28. DEGRA Output Power for Nominal Insulation and Hi Rate Resistance Change for Varying Coating Lifetimes

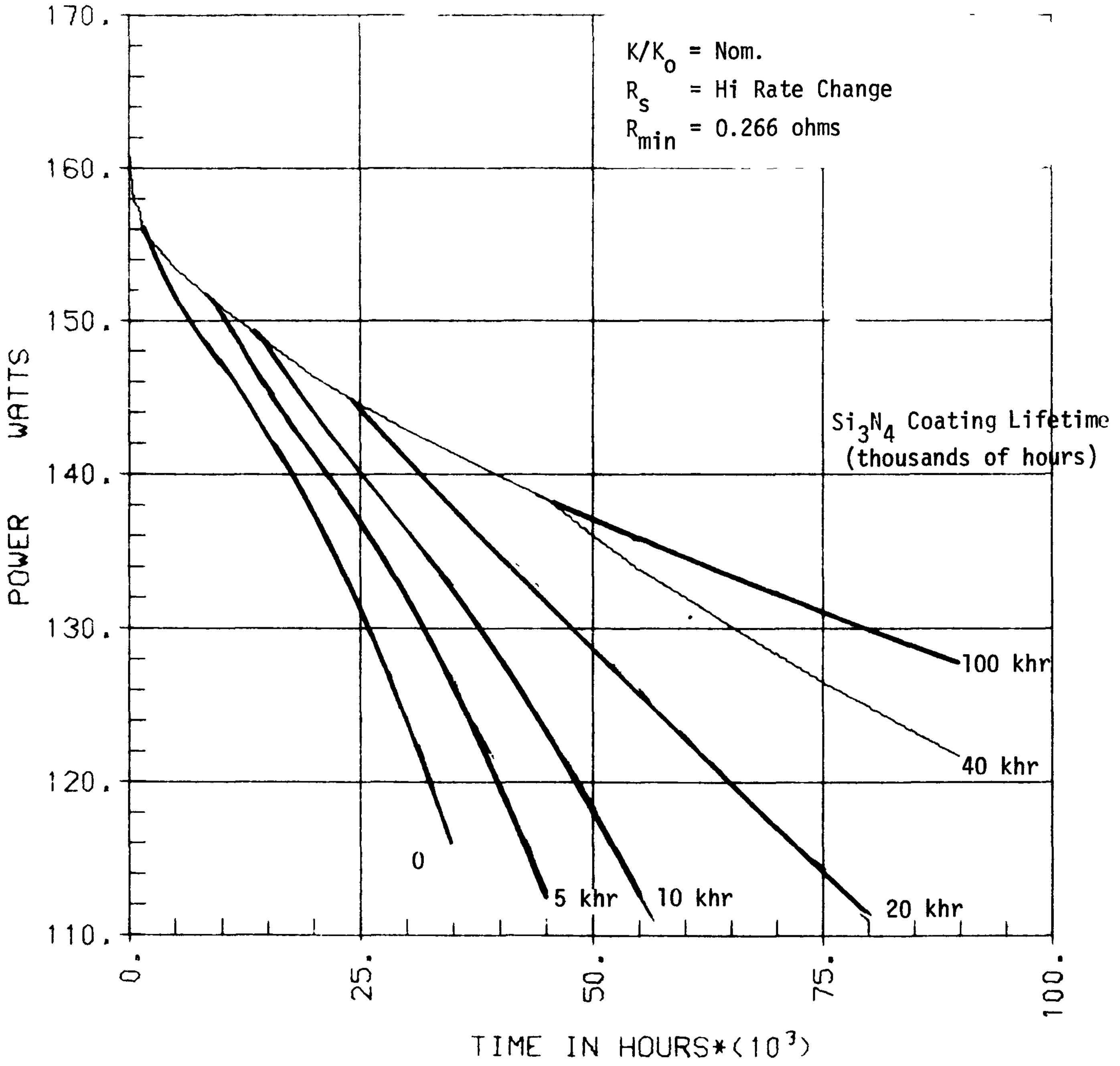

Figure 29. DEGRA Output Power for Nominal Insulation and Hi Rate Resistance Change Having R_{min} of 3.46 ohms

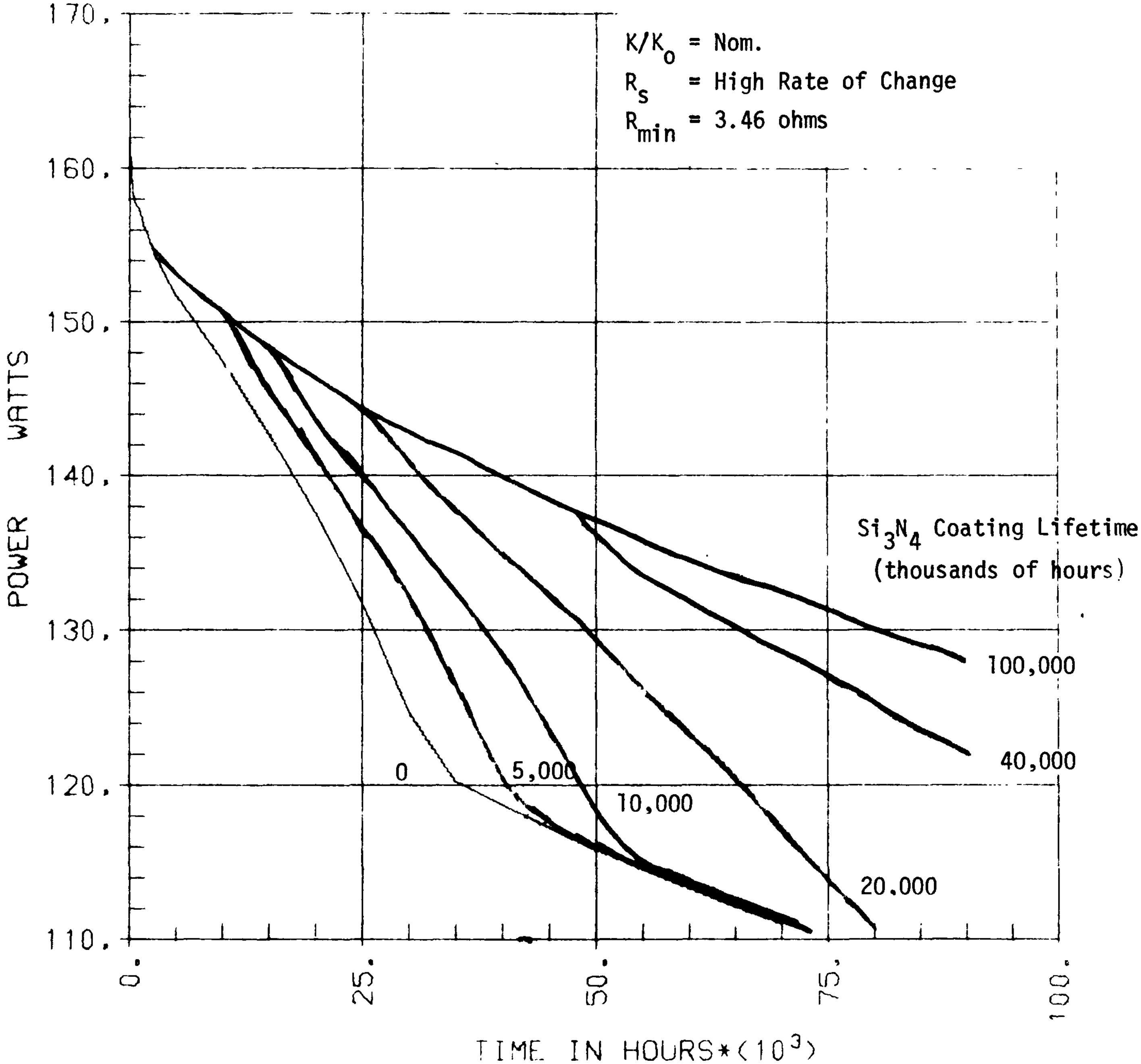

Figure 30. DEGRA Output Power for Nominal Insulation and Hi Rate Resistance Change Having R_{min} of 4.78 ohms

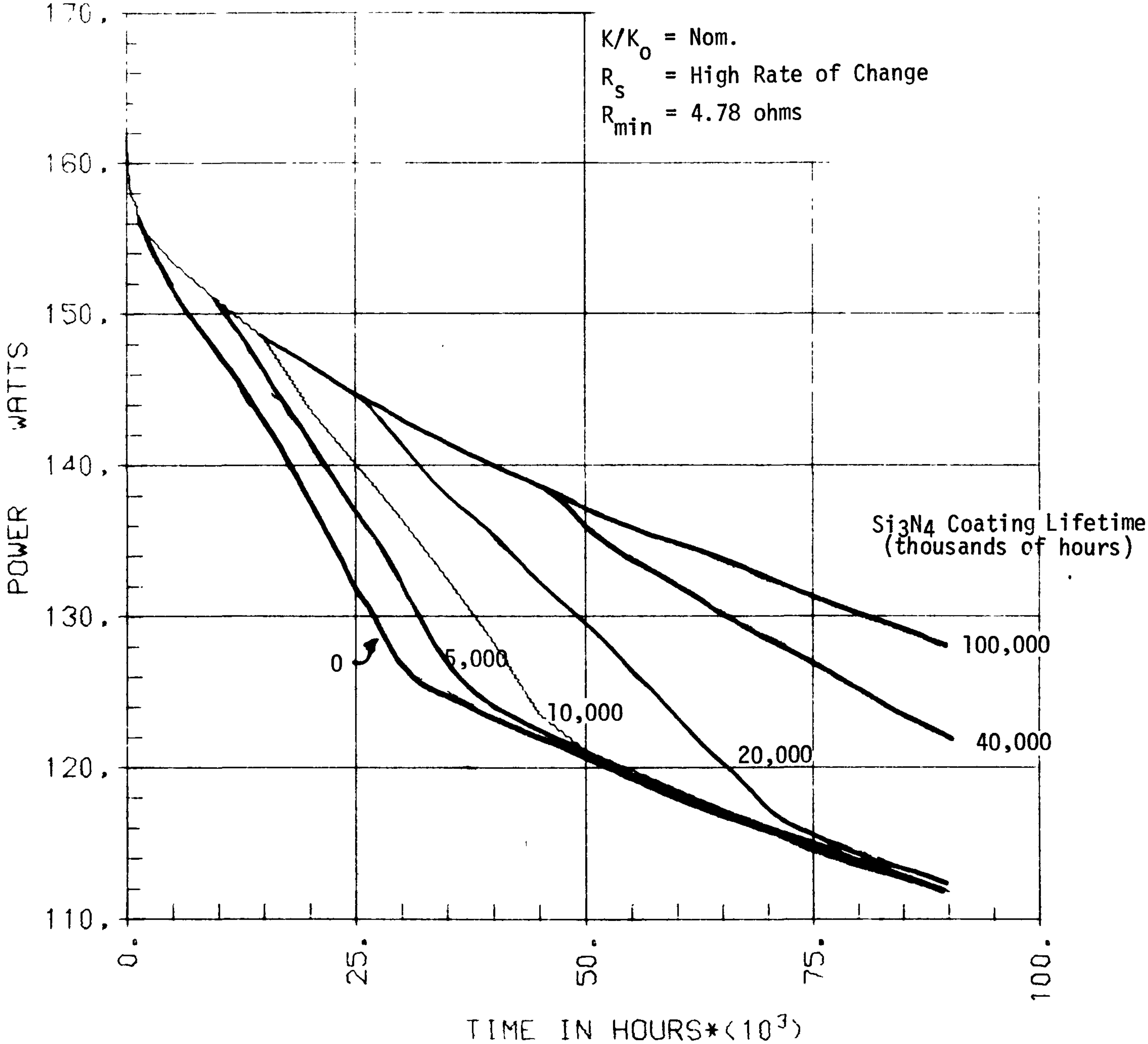

resistances. The drastic effect which the minimum shunt resistance has on the available output power is clearly demonstrated in these three figures. Should the worst case prevail, i.e., little or no limit in shunt resistance (R_{min} = 0.266 ohms), a catastrophic failure of the generator is possible if the Si_3N_4 coating does not remain intact throughout the mission. However, as indicated earlier, the most likely value of minimum shunt resistance is between 3.5 and 5 ohms.

The effect of an increased beginning of life heat source fuel loading was also considered. The fuel load was increased by 40 watts (thermal) from 2360 watts to 2400 watts. This increase affects the available power output in several ways. Initially, the output power will be increased due to the increased hot junction temperatures (the hot junction temperature will increase by 12°C for the 40 watt increase in thermal input power). This elevated temperature, however, will also increase the rate at which the degradation mechanisms occur. In addition, the lifetime of the Si_3N_4 coatings is reduced by the increased temperature. For example, if an internal CO pressure of 1×10^{-5} Torr is assumed, then the Si_3N_4 coating lifetime (at 1000°C) is reduced from 36,000 hours to 23,000 hours at a hot junction temperature of 1012°C. (See Figure 12, assuming a constant BOL temperature). Under the assumption that the coating lifetime is at least 100,000 hours, it is seen from Figure 31 that increasing the BOL temperature by 12°C results in greater power ($\sim$ 3 watts) for all lifetimes out to at least 90,000 hours. Thus, the higher degradation mechanisms which are at work do not affect performance for just a 12°C increased temperature. However, if a lower coating lifetime is considered, e.g., the assumption is made that the coating will come off after 40,000 hours (for 1000°C hot junction temperature) and after 20,000 hours for the case of operating 12°C higher, then the increased BOL temperature has a rather drastic effect on the generator performance. Figures 32 and 33 show the generator performance under the above

Figure 31. DEGRA Output Power for Nominal Insulation and Resistance Change for Different BOL Temperatures While Continuously Coated

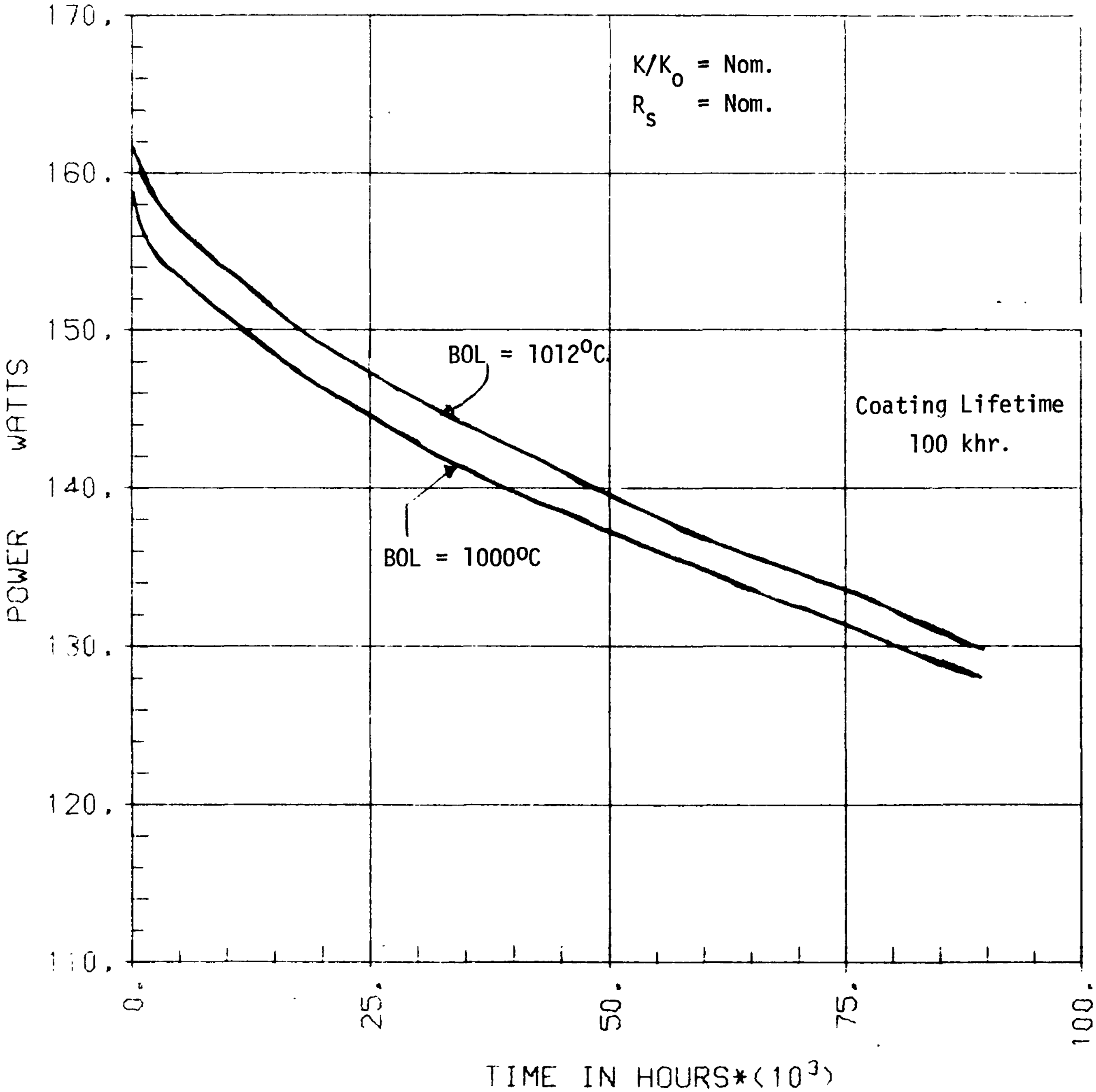

Figure 32. DEGRA Output Power for Nominal Insulation and Resistance Change for Different BOL Temperatures with Loss of Si_3N_4 Coating

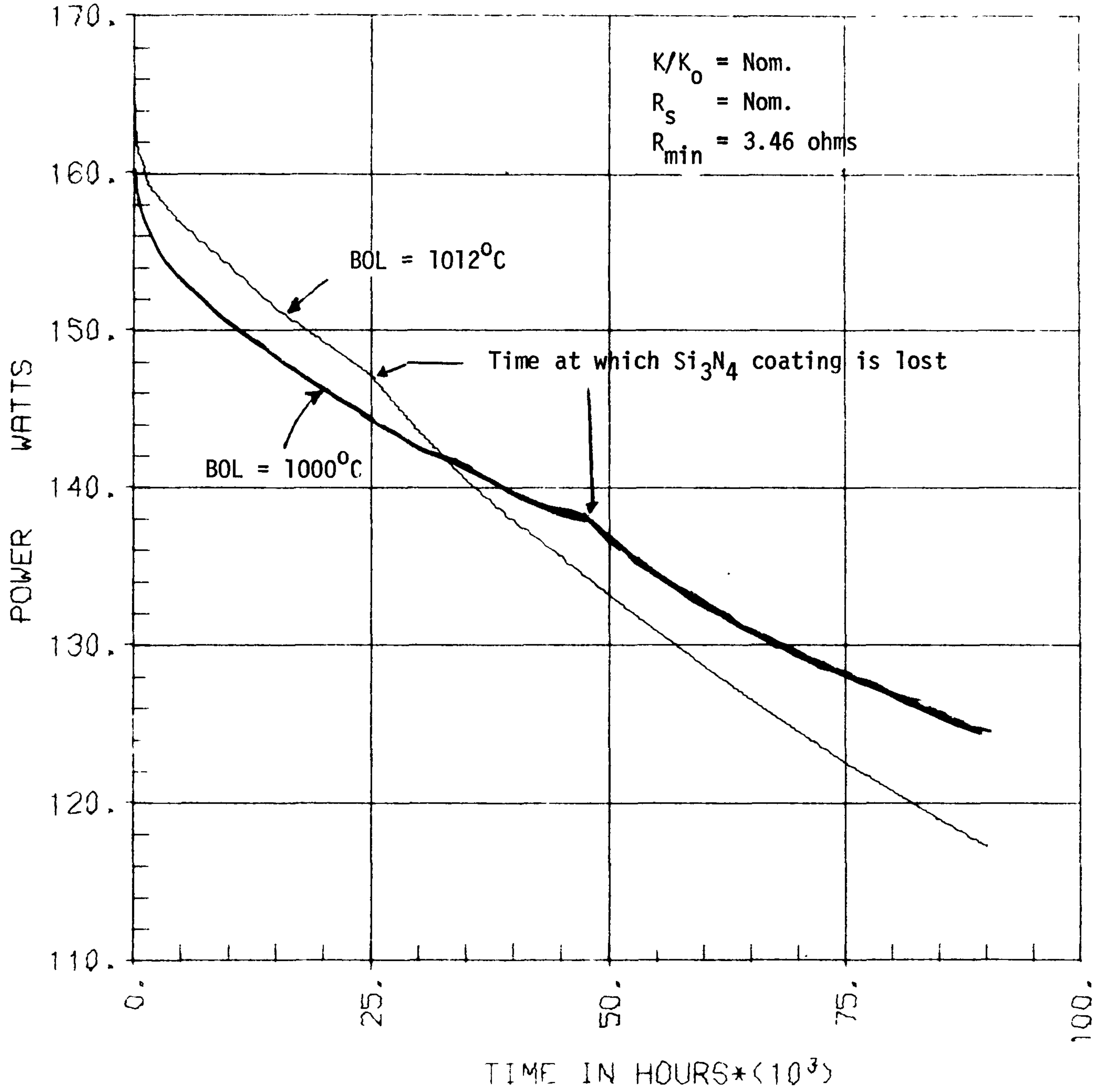

Figure 33. DEGRA Output Power for Nominal Insulation Change, High Rate Resistance Change for Different BOL Temperatures with Loss of Si_3N_4 Coating

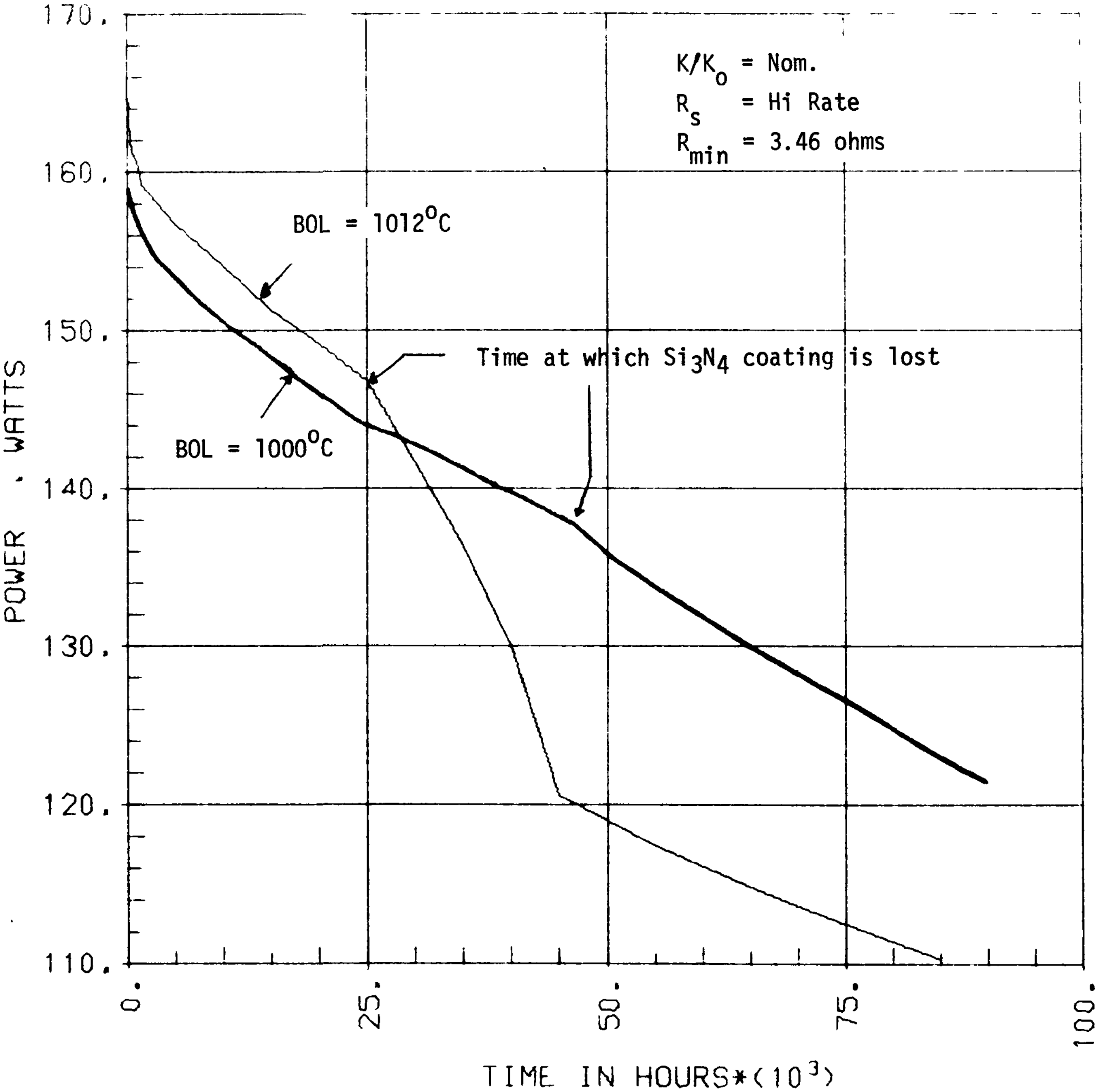

assumptions for the nominal degradation rate change and the case where the shunt resistance changes at the high rate. Under these conditions, it can be seen that the increased fuel loading will result in 2 to 10 watts lower output power after 40,000 hours, depending upon the degradation rate which is used. Actually, it is expected that with a BOL temperature of 1012^{o}C the coating lifetime will be at least 30,000 hours. (The 20,000 hours is based on a 10^{-5} Torr CO pressure and a constant hot junction temperature of 1012^{o}C. During the mission, the operating temperature will decrease about 15^{o}C after 20,000 hours.) Therefore, the power at 40,000 hours should be nearly the same no matter which level of fuel loading is selected. Certainly, the lower level is preferred for safety.

SECTION XI

COMPARISON OF FLIGHT RTGs (LES 8 AND LES 9) WITH THE DEGRA COMPUTER CODE PREDICTION

The accuracy of the performance predictions given in the previous sections and the confidence one places in the correctness of these projections depend ultimately on the congruence of the predicted versus actual generator performance. Conversely, once having proven the accuracy of the model, the confidence that a given RTG is performing "nominally" is greatly enhanced if its performance follows the predictions made by the model.

The RTGs powering the LES 8 and 9 spacecrafts are the first flight generators of this type (the type which utilizes the SiGe thermoelectric technology) to be flown. A couple of minor adjustments to the normal operational mode of the DEGRA code were required to make it compatible with the LES 8 and 9 RTGs. This entailed reduction of the load voltage (i.e., the LES 8 and 9 output voltages are 26.5 volts as compared to the 30 volt output of the MJS RTGs) and a change of the ambient sink temperature (the MJS trajectory is a motion away from the sun, while the LES 8 and 9 are earth orbiters). The earth orbiting mission trajectory of the LES 8 and 9 spacecrafts produce the additional anomaly of a sinusoidal temperature profile with a resultant daily hot and cold junction temperature fluctuation of 20^{o}C. Most all of the degradation mechanisms which occur in an RTG (other than fuel decay) are strongly dependent upon operating temperatures. For this reason, DEGRA computer runs were made for two levels of temperature: a) the high temperature condition which conservatively simulates the continuous operation of the generator at the daily peak temperature ($T_{hot\ junction} = 990^{o}C$ at BOL) and b) at an average temperature corresponding to the daily average temperature recordings ($T_{hot\ junction} = 980^{o}C$ at BOL).

For each of these two temperature conditions, the code was exercised in two different degradation modes: 1) nominal rate of change for insulation and shunt resistance changes and 2) nominal rate of change for insulation changes and the high rate of change for shunt resistance changes. The protective Si_3N_4 coating (this coating is also utilized for the LES 8 and 9 generator unicouples) is assumed to be intact throughout the projected operating time (90,000 hours).

The results of this computer output showed that the generator output power profile was identical for both degradation modes (nominal or high rate change), because in neither case did the generator lose power due to shunt resistance. The two different temperature levels of course resulted in two different output power levels. Table 1 to 4 show the output power of the generator (last column on each table) up to the 90,000 hours of operating time for the four different cases which were run.

The major difficulty in comparing the performance of the flight generators with the DEGRA predicted performance results is in estimating the "age" of the RTG at beginning of mission (BOM). For this comparison, several different ages at BOM were assumed. To simplify the task further, the ratio of the output powers (i.e., the output power divided by the initial output power) is compared rather than the measured or calculated output powers. Figure 34 shows this comparison. The DEGRA predictions were determined for three different ages at BOM, i.e., 1500 hours, 1000 hours and 500 hours. The four flight generators were then plotted on the same graph, using launch time as zero or initial operating time. The degradation modes of three of the four generators are almost identical and fall within less than 0.5% of the DEGRA prediction labeled "1500h DEGRA". This would indicate that these three generators were launched with an equivalent "age" of 1500 hours, while it appears that the fourth generator is performing as a "younger" generator, i.e., indicating an equivalent age at launch of somewhere between 500 and 1000 hours. The primary contractor for the generators, General

Table 1.

XXXXXXXXXXXXXXXXXXXXXXXXXXXXXXXXXXXXXXXXXXXXXXXXX
X ELECTRICAL PERFORMANCE CHARACTERISTICS. X
XXXXXXXXXXXXXXXXXXXXXXXXXXXXXXXXXXXXXXXXXXXXXXXXX

TIME (HOURS)	CURRENT (AMPERES /COUPLE)	OPEN CIRCUIT VOLTAGE (V/COUPLE)	Q(HS) (W/COUPLE)	SHUNT POWER LOSS(W/GEN)	OUTPUT POWER (W/GEN)
0.	3.018	.323	7.560+00	7.6903-02	159.98
10.	3.009	.328	7.560+00	7.6903-02	159.48
100.	2.969	.340	7.559+00	7.6903-02	157.40
500.	2.916	.351	7.557+00	7.6903-02	154.56
1000.	2.905	.356	7.553+00	7.6903-02	153.98
1500.	2.867	.360	7.550+00	7.6903-02	151.96
3000.	2.841	.365	7.540+00	7.6903-02	150.60
5000.	2.790	.370	7.526+00	7.6903-02	147.92
10000.	2.733	.375	7.493+00	7.6903-02	144.86
15000.	2.688	.377	7.459+00	7.6903-02	142.49
20000.	2.648	.378	7.426+00	7.6903-02	140.38
25000.	2.614	.378	7.393+00	7.6903-02	138.58
30000.	2.584	.378	7.360+00	7.6903-02	136.97
35000.	2.556	.377	7.327+00	7.6903-02	135.50
40000.	2.531	.377	7.295+00	7.6903-02	134.14
45000.	2.506	.376	7.262+00	7.6903-02	132.84
50000.	2.481	.375	7.230+00	7.6903-02	131.54
55000.	2.458	.375	7.198+00	7.6903-02	130.30
60000.	2.436	.374	7.166+00	7.6903-02	129.12
65000.	2.414	.373	7.134+00	7.6903-02	127.99
70000.	2.394	.372	7.102+00	7.6903-02	126.89
75000.	2.375	.371	7.070+00	3.1163-02	125.88
80000.	2.355	.370	7.039+00	3.2794-02	124.85
85000.	2.337	.369	7.007+00	3.4295-02	123.86
90000.	2.318	.368	6.976+00	3.5673-02	122.89

$T_{c\ jct}$ = 300°C/orbit

K/K_o = Nominal

R_{shunt} = Nominal

V_{out} = 26.5 V

R_{min} = 0.2665 ohms

Table 2.

XXXXXXXXXXXXXXXXXXXXXXXXXXXXXXXXXXXXXXXXXXXXXXXXXX
X ELECTRICAL PERFORMANCE CHARACTERISTICS. X
XXXXXXXXXXXXXXXXXXXXXXXXXXXXXXXXXXXXXXXXXXXXXXXXXX

TIME (HOURS)	CURRENT (AMPERES /COUPLE)	OPEN CIRCUIT VOLTAGE (V/COUPLE)	Q(HS) (W/COUPLE)	SHUNT POWER LOSS(W/GEN)	OUTPUT POWER (W/GEN)
0.	3.018	.323	7.560+00	7.6903-02	159.98
10.	3.009	.328	7.560+00	7.6903-02	159.48
100.	2.969	.340	7.559+00	7.6903-02	157.40
500.	2.916	.351	7.557+00	7.6903-02	154.56
1000.	2.905	.356	7.553+00	7.6903-02	153.98
1500.	2.867	.360	7.550+00	7.6903-02	151.96
3000.	2.841	.365	7.540+00	7.6903-02	150.60
5000.	2.790	.370	7.526+00	7.6903-02	147.92
10000.	2.733	.375	7.493+00	7.6903-02	144.86
15000.	2.688	.377	7.459+00	7.6903-02	142.49
20000.	2.648	.378	7.426+00	7.6903-02	140.38
25000.	2.614	.378	7.393+00	7.6903-02	138.58
30000.	2.584	.378	7.360+00	7.6903-02	136.97
35000.	2.556	.377	7.327+00	7.6903-02	135.50
40000.	2.531	.377	7.295+00	7.6903-02	134.14
45000.	2.506	.376	7.262+00	7.6903-02	132.84
50000.	2.481	.375	7.230+00	7.6903-02	131.54
55000.	2.458	.375	7.198+00	7.6903-02	130.30
60000.	2.436	.374	7.166+00	7.6903-02	129.12
65000.	2.414	.373	7.134+00	7.6903-02	127.99
70000.	2.394	.372	7.102+00	7.6903-02	126.89
75000.	2.374	.371	7.070+00	5.8386-02	125.86
80000.	2.355	.370	7.039+00	6.2792-02	124.83
85000.	2.336	.369	7.007+00	6.6939-02	123.83
[illegible]	2.318	.368	6.976+00	7.0815-02	122.86

$T_{c\ jct}$ = 300°C/orbit

K/K_o = Nominal

R_{shunt} = High Rate of Change

V_{out} = 265 V

R_{min} = 0.266 ohms

900-755

Table 3.

XXXXXXXXXXXXXXXXXXXXXXXXXXXXXXXXXXXXXXXXXXXXXX
X ELECTRICAL PERFORMANCE CHARACTERISTICS. X
XXXXXXXXXXXXXXXXXXXXXXXXXXXXXXXXXXXXXXXXXXXXXX

TIME (HOURS)	CURRENT (AMPERES /COUPLE)	OPEN CIRCUIT VOLTAGE (V/COUPLE)	Q(HS) (W/COUPLE)	SHUNT POWER LOSS(W/GEN)	OUTPUT POWER (W/GEN)
0.	3.042	.322	7.560+00	7.6903-02	161.24
10.	3.031	.327	7.560+00	7.6903-02	160.67
100.	2.991	.339	7.559+00	7.6903-02	158.55
500.	2.937	.350	7.557+00	7.6903-02	155.67
1000.	2.929	.355	7.553+00	7.6903-02	155.27
1500.	2.887	.359	7.550+00	7.6903-02	153.03
3000.	2.865	.364	7.540+00	7.6903-02	151.87
5000.	2.810	.369	7.526+00	7.6903-02	148.95
10000.	2.752	.374	7.493+00	7.6903-02	145.86
15000.	2.708	.376	7.459+00	7.6903-02	143.52
20000.	2.670	.377	7.426+00	7.6903-02	141.52
25000.	2.636	.377	7.393+00	7.6903-02	139.72
30000.	2.606	.377	7.360+00	7.6903-02	138.12
35000.	2.578	.377	7.327+00	7.6903-02	136.66
40000.	2.552	.376	7.295+00	7.6903-02	135.30
45000.	2.528	.376	7.262+00	7.6903-02	134.00
50000.	2.503	.375	7.230+00	7.6903-02	132.71
55000.	2.480	.374	7.198+00	7.6903-02	131.48
60000.	2.458	.373	7.166+00	7.6903-02	130.30
65000.	2.437	.373	7.134+00	7.6903-02	129.17
70000.	2.416	.372	7.102+00	7.6903-02	128.08
75000.	2.396	.371	7.070+00	7.6903-02	127.03
80000.	2.377	.370	7.039+00	7.6903-02	126.01
85000.	2.358	.369	7.007+00	7.6903-02	125.01
90000.	2.340	.368	6.976+00	7.6903-02	124.05

$T_{c\ jct}$ = 290°C/orbit

K/K_o = Nominal

R_{shunt} = Nominal

V_{out} = 26.5 V

R_{min} = 0.266 ohms

Table 4.

XXXXXXXXXXXXXXXXXXXXXXXXXXXXXXXXXXXXXXXXXXXXXXXXXX
X ELECTRICAL PERFORMANCE CHARACTERISTICS. X
XXXXXXXXXXXXXXXXXXXXXXXXXXXXXXXXXXXXXXXXXXXXXXXXXX

TIME (HOURS)	CURRENT (AMPERES /COUPLE)	OPEN CIRCUIT VOLTAGE (V/COUPLE)	Q(HS) (W/COUPLE)	SHUNT POWER LOSS(W/GEN)	OUTPUT POWER (W/GEN)
0.	3.042	.322	7.560+00	7.6903-02	161.24
10.	3.031	.327	7.560+00	7.6903-02	160.67
100.	2.991	.339	7.559+00	7.6903-02	158.55
500.	2.937	.350	7.557+00	7.6903-02	155.67
1000.	2.929	.355	7.553+00	7.6903-02	155.27
1500.	2.887	.359	7.550+00	7.6903-02	153.03
3000.	2.865	.364	7.540+00	7.6903-02	151.87
5000.	2.810	.369	7.526+00	7.6903-02	148.95
10000.	2.752	.374	7.493+00	7.6903-02	145.86
15000.	2.708	.376	7.459+00	7.6903-02	143.52
20000.	2.670	.377	7.426+00	7.6903-02	141.52
25000.	2.636	.377	7.393+00	7.6903-02	139.72
30000.	2.606	.377	7.360+00	7.6903-02	138.12
35000.	2.578	.377	7.327+00	7.6903-02	136.66
40000.	2.552	.376	7.295+00	7.6903-02	135.30
45000.	2.528	.376	7.262+00	7.6903-02	134.00
50000.	2.503	.375	7.230+00	7.6903-02	132.71
55000.	2.480	.374	7.198+00	7.6903-02	131.48
60000.	2.458	.373	7.166+00	7.6903-02	130.30
65000.	2.437	.373	7.134+00	7.6903-02	129.17
70000.	2.416	.372	7.102+00	7.6903-02	128.08
75000.	2.396	.371	7.070+00	7.6903-02	127.03
80000.	2.377	.370	7.039+00	7.6903-02	126.01
85000.	2.358	.369	7.007+00	7.6903-02	125.01
90000.	2.340	.368	6.976+00	7.6903-02	124.05

$T_{c\ jct}$ = 290°C/orbit

K/K_o = Nominal

R_{shunt} = High Rate of Change

V_{out} = 26.5 V

R_{min} = 0.266 ohms

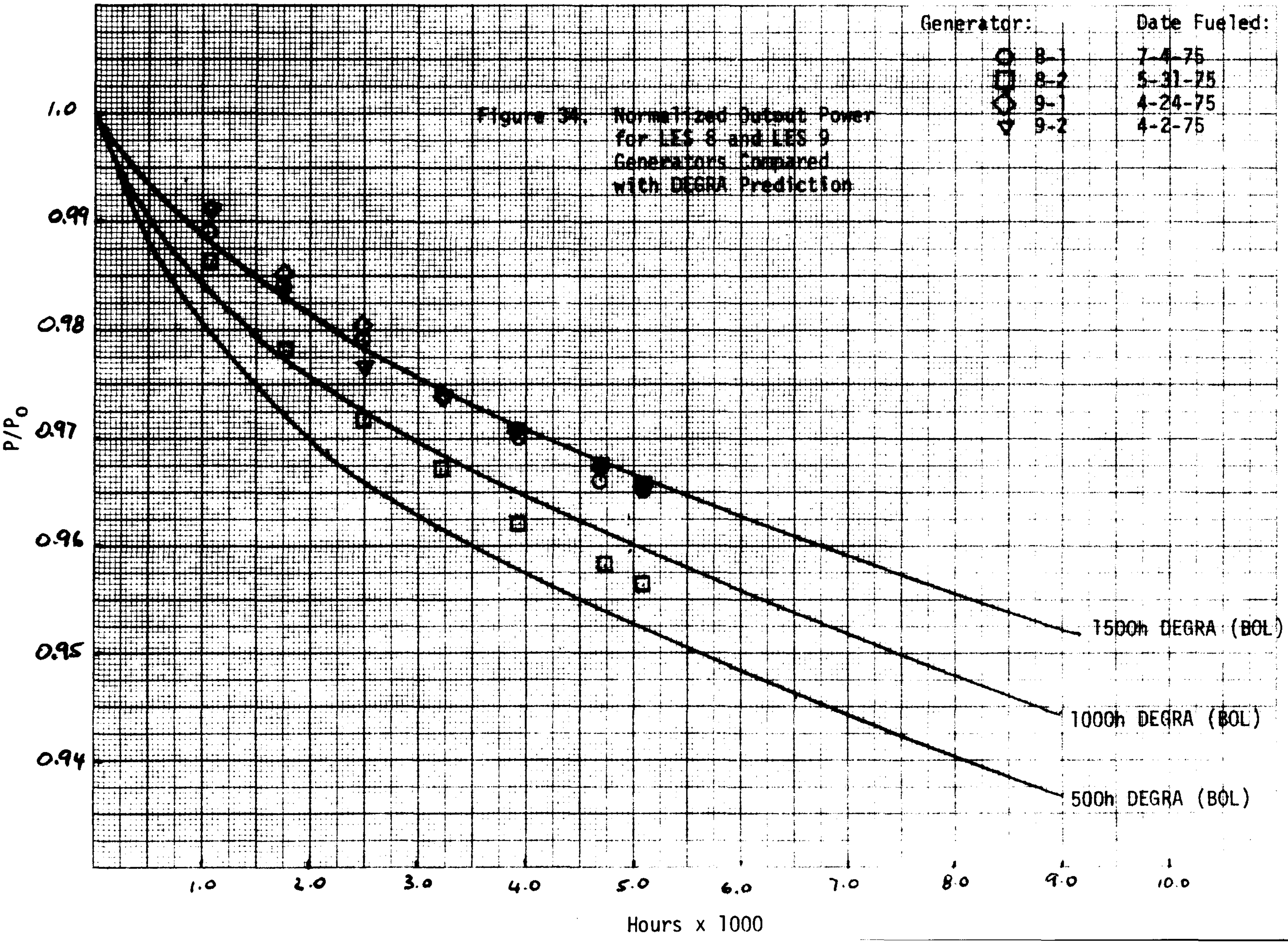

Figure 34. Normalized Output Power for LES 8 and LES 9 Generators Compared with DEGRA Prediction

900-755

Electric Company, was queried as to the history of the four generators. They indicated that at the present time, a compilation of the temperature-time status of all four generators is being conducted, the results of which will be made available to JPL as soon as their study is completed. For the present time, GE is using an "equivalent" age at BOM of 800 hours, which, based on the data shown in the figure, is somewhat on the conservative side.

SECTION XII

CONCLUSIONS

A number of degradation mechanisms, relating to property changes, chemical reactions, isotope decay, etc., significantly reduce the output power from an RTG. These mechanisms have been examined and described in detail. Their synergetic interactions have been evaluated by means of the computer code DEGRA, and an estimate of the available output power from an RTG as a function of mission time has been made. The results of this program show that provided 1) a minimum shunt resistance limit of about 3 to 4 ohms per generator exists or 2) the Si_3N_4 coating lifetime exceeds the required mission time, no catastrophic failure of the RTG is anticipated due to any of the presently known mechanisms. The results further show that under the most likely worst case conditions anticipated at the present time (e.g., k/k_0 = nom, R_s = high rate, coating lifetime = 10,000 hrs) a minimum output power of 128 watts per generator can be expected at the end of a 40,000 hour space flight mission. (This assumes a BOL value of about 156 watts.) Also, with the present understanding of the effect of the various degradations, a nominal output power of 140 watts per generator will be available at end of mission. This amount of available output power can be reduced, however, by 2 to 10 watts even for the nominal conditions if an excess fuel loading is used and if the Si_3N_4 coating deteriorates before the end of the mission.

The conclusion which can be drawn from the comparison with the flight generators is that the DEGRA prediction (using a 1500 hours age at BOM) is very close to the actual performance of three of the four LES generators. The fact that one of the four generators is not performing as expected may easily be explainable by a different time-temperature history (different age) of this generator. It should also be kept in mind that the difference in this generator is really very small (less than 1%), and its degradation trend does appear to be parallel to the remaining generators.

SECTION XIII

REFERENCES

1. V. Raag, "Mathematical Model and Computer Program for the Design and Analysis of Silicon Germanium Air Vac RTGs," Memo #14, Syncal Corp., Sept. 1971.
2. G. Stapfer and V. C. Truscello, "A Model to Predict the Degradation of a SiGe Thermopile," 7th IECEC, San Diego, CA, 1972.
3. "Silicon Germanium Technology Program Report No. 2," JPL Internal Report 900-629, August 1973.
4. G. Stapfer, "Performance Prediction of the Multihundred Watt (MHW) Radioisotope Thermoelectric Generator (RTG)," JPL Internal Report EM 342-279, Dec. 1974.
5. G. Stapfer and E. L. Noon, "Performance Prediction of the Mulithundred Watt (MHW) Radioisotope Thermoelectric Generator (RTG) Using Si_3N_4 Coated Unicouples," JPL Internal Report EM 342-314, Aug. 1975.
6. E. L. Noon and G. Stapfer, "A Computer Program Designed for the Reduction of Eighteen-Couple Module Test Data," JPL Internal Report 900-690, Dec. 1974.
7. G. Stapfer and V. C. Truscello, "The Long - Term Performance Degradation of a Radioisotope Thermoelectric Generator Using Silicon Germanium," 11th IECEC, Lake Tahoe, Nev., Sept. 1976.
8. Bimonthly Progress Report, "Multihundred Watt Radioisotope Thermoelectric Generator Program LES 8/9 Program, MJS Program, Period 1 May - 30 June 1975," pages 6-46, General Electric Company.